Intelligent Control and Automation, 2026, 17(4), 235-269
https://www.scirp.org/journal/ica
ISSN Online: 2153-0661
ISSN Print: 2153-0653

A Hybrid Probabilistic Framework for Managing Systemic Risks in Human-Centric Wearables-Enabled Manufacturing

Ali Karevan, Sylvie Nadeau

École de technologie supérieure, Mechanical Engineering Department, Montreal, Quebec, Canada
Email: ali.karevan.1@ens.etsmtl.ca, sylvie.nadeau@etsmtl.ca

How to cite this paper: Karevan, A. and Nadeau, S. (2026) A Hybrid Probabilistic Framework for Managing Systemic Risks in Human-Centric Wearables-Enabled Manufacturing. *Intelligent Control and Automation*, **17**, 235-269.
https://doi.org/10.4236/ica.2026.174012

Received: September 16, 2026
Accepted: November 6, 2026
Published: November 9, 2026

Copyright © 2026 by author(s) and Scientific Research Publishing Inc.
This work is licensed under the Creative Commons Attribution-NonCommercial International License (CC BY-NC 4.0).
http://creativecommons.org/licenses/by-nc/4.0/



Open Access

Abstract

This paper proposes a novel hybrid framework, STPA-BN-PSO, designed to proactively quantify and manage systemic sociotechnical risks in wearables-enabled manufacturing. The study specifically addresses the "parameterization gap" that occurs during the design and early integration phases when empirical failure data for new technologies is scarce. The methodology integrates System-Theoretic Process Analysis (STPA) to derive hierarchical control structures, Bayesian Networks (BN) for probabilistic modeling, and Particle Swarm Optimization (PSO) to calibrate weighted conditional probability tables against expert-derived profiles. The framework is validated through three distinct Industry 5.0 case studies: sequential assembly, flexible job-shop, and disassembly for recycling. This research provides a unique contribution by positioning PSO as a calibration engine for STPA-derived structures. Unlike traditional data-driven BNs, this framework allows for path-based probabilistic quantification and predictive risk assessment before a system becomes operational, bridging the gap between qualitative systems-thinking and quantitative reliability engineering. Results demonstrate that operational vulnerability is highly context-dependent, with the flexible job-shop showing the highest baseline risk (31.5%). Criticality analysis identifies shifting risk drivers: planning quality dominates sequential assembly (ΔRisk = 0.181), while digital information quality is the primary amplifier in flexible job-shops (ΔRisk = 0.286). Sensitivity analyses reveal that risk-propagation pathways reorganize significantly based on operational layout.

Keywords

Bayesian Networks, Particle Swarm Optimization, Systemic Risk, STPA, Industry 5.0, Wearables-Enabled Manufacturing

1. Introduction

The manufacturing world is evolving, increasingly shaped by Industry 4.0 technologies [1] and the push towards a more human-centric vision of Industry 5.0 [2] [3]. A key part of this evolution involves integrating smart wearables, like smart glasses [4] and gloves, directly into workflows. These devices hold significant promises: providing workers with real-time data, enhancing safety awareness, and potentially streamlining complex tasks such as hybrid assembly and disassembly [5]. However, the introduction of these devices comes with different types of risks and challenges [6] [7]. Potential human-system interaction errors, data security vulnerabilities, device reliability issues, and unforeseen consequences arising from the interplay between multiple wearables and existing systems are some of these sociotechnical risks that directly impact system reliability [8] [9]. Thus, developing effective methods for assessing and managing these risks is becoming critical for the safe and successful adoption of wearable technology in manufacturing [10] [11].

Traditional risk techniques struggle to capture the dynamic, interconnected, and uncertain nature of modern sociotechnical risks [12] [13]. As a result, there is a growing demand for systemic and quantitative models that navigate this complexity and support risk-informed decisions [14]. BNs have emerged as a particularly well-suited approach for such scenarios. While BNs are powerful for modeling complex causal relationships under uncertainty [15]-[19], standard data-driven BNs often lack a systemic foundation for identifying safety boundaries before empirical data exists. BNs allow for the integration of diverse information sources, including historical data, sensor readings, and expert knowledge. They are particularly strong to analyze multifaceted risk factors in areas ranging from infrastructure management and supply chains to healthcare predictions and fault diagnosis [20]-[23]. The ability to revise probabilities with new evidence enhances BNs for dynamic risk assessment in changing environments [15] [24]-[28].

While BNs provide a strong foundation for modeling risk probabilities, their effectiveness in sociotechnical systems is heavily dependent on the structural validity of the network [29] [30]. In this context, STPA provides a critical systemic view, allowing for the identification of causal relationships based on hierarchical control loops and feedback failures rather than purely statistical correlations [14]. By anchoring the BN architecture in the systemic outputs of STPA, the model captures a top-down perspective of safety boundaries. Once this foundational structure is established, optimizing the analysis benefits from complementary techniques like PSO. PSO, a population-based metaheuristic algorithm inspired by social behaviors, has proven highly effective in navigating complex, high-dimensional search spaces to find near-optimal solutions [31] [32]. Its flexibility and practicality have led to its successful application across various domains, often in conjunction with other modeling techniques (including BNs) for tasks such as parameter optimization, calibration of CPTs, network structure learning, and efficient resource allocation [17] [30] [33]-[35].

However, despite the capabilities of BN and PSO, a notable gap exists in the analysis of systemic risks introduced by modern digital tools, such as smart wearables, within complex operational contexts. Specifically, a critical challenge lies in the proactive assessment of systemic risks during the design and early integration phases, where empirical failure data for new wearable technologies is often nonexistent. It remains unclear how to objectively calibrate probabilistic models under these conditions or how risk propagation pathways will reorganize across different Industry 5.0 layouts. To address this, this study proposes a hybrid STPA-BN-PSO method designed to systemically manage and predict the risks of integrating smart glasses [4] and gloves in assembly/disassembly processes from the earliest design stages through to operation. This research aims to answer:

1) How can systemic human-wearable risks be structured into a hierarchical probabilistic model?

2) How can PSO reduce subjectivity in BN calibration under data uncertainty?

3) How do critical risk drivers differ across diverse manufacturing contexts?

The primary contribution of this work is a novel STPA-BN-PSO framework that anchors the BN structure in system theory to address the "parameterization gap." Unlike existing hybrids like STPA-PSO [14], which focuses on prioritization, or FRAM-PSO [36], which manages operational variability, this framework provides a path-based, probabilistic quantification of risk reorganization specifically during the design phase.

The rest of the paper is organized as follows. Section 2 reviews related work; Section 3 details the STPA-BN-PSO methodology; Section 4 presents results; Section 5 discusses implications and limitations; Section 6 concludes.

2. Literature Review and Research Context

Modeling complex systems with inherent uncertainty is a persistent challenge in fields ranging from engineering to finance. To address this, researchers have increasingly turned to probabilistic graphical models. Among these, Bayesian Networks, which are founded on Bayes' theorem as shown in Equation (1), are considered one of the most effective theoretical models for illustrating relationships between system variables amidst uncertainty [37] [38]:

$$P(A|E) = \frac{P(E|A)P(A)}{P(E)} \tag{1}$$

As a combination of probability, graph, and decision theory, BNs offer a powerful graphical framework for probabilistic reasoning [39] [40]. Their distinct advantages include a high tolerance for incomplete data and the ability to represent complex interdependencies, including those with common causal factors [41] [42]. However, in the context of Industry 5.0, the risks associated with smart wearables are predominantly sociotechnical, involving cognitive load, human-machine interface (HMI) distractions, and data privacy concerns [7] [8]. While traditional BNs have been used for mechanical reliability (based on component-level break-

downs), their application to these emerging systemic wearable-driven risks requires a structure that can account for systemic control failures.

A significant challenge in BN modeling lies in constructing the network itself. While domain experts can define some dependencies, learning the BN structure from large datasets is often preferred. Modern research has proposed various approaches, including constraint-based methods (e.g., PC or IC algorithms), score-based methods, and more recently, Deep Bayesian Networks that utilize neural architectures to capture higher-order dependencies [43] [44]. However, such data-driven methods are inherently inapplicable during the design and early integration phases of emergent technologies—such as Industry 5.0 smart wearables—where historical failure data is non-existent or extremely scarce. Relying on historical data for proactive safety is a fundamental limitation; therefore, this study addresses this "data-gap" by using STPA to define the causal structure based on hierarchical control logic rather than statistical history. By anchoring the BN in STPA, the model moves beyond purely statistical correlations to reflect the actual functional architecture of the manufacturing system. Crucially, this enables the framework to predict how risk propagation pathways reorganize when system layouts or control strategies are modified during the design phase. This provides a proactive, safety-guided assessment tool that identifies systemic vulnerabilities before the manufacturing process becomes operational, filling a gap that purely data-driven models cannot address.

Once the structure is defined, the secondary challenge is the calibration of CPTs. Finding the optimal parameters for a BN is an NP-hard problem. While Genetic Algorithms (GA) and Simulated Annealing (SA) have been used, they are often prone to becoming trapped in local optima and can lack the efficiency required for complex datasets [44]. Therefore, PSO has gained significant attention as a heuristic search method for parameter learning. Its appeal lies in its effectiveness at locating global optima and its relatively straightforward implementation, leading numerous researchers to combine PSO with BN to solve diverse problems [17] [24] [44]-[46].

While the combination of BN and PSO has been explored in other domains, such as healthcare and supply chain optimization [17] [30], a notable gap exists in its application to systemic, path-based risk assessment. Most existing BN-PSO models use PSO for structure learning; in contrast, this study utilizes PSO to solve the "parameterization gap" specifically during the design and early integration phases, where low-level empirical data is naturally unavailable. By calibrating CPTs against high-level systemic risk profiles, the framework can quantify how a localized wearable failure propagates into a system-wide loss before the system is physically operational. By positioning the BN-PSO framework as a calibration engine for STPA-derived structures, this research provides a novel solution for predicting how risk pathways reorganize as different design configurations or manufacturing layouts are considered. This enables the management of emergent risks in Industry 5.0 through a proactive, logic-based approach rather than relying on

retrospective historical data.

3. Methodology

This study introduces a hybrid STPA-BN-PSO framework designed to quantify and manage systemic risks in wearables-enabled manufacturing. The methodology is organized into four distinct stages:

- Qualitative hazard identification: Utilizing STPA to define the causal structure and control loops. While Fault tree analysis (FTA) is a common starting point for this task in the literature [47], it struggles to adequately model the complex interdependencies and feedback loops characteristic of modern sociotechnical systems [48].
- Probabilistic mapping: Translating STPA outputs into a three-tiered hierarchical Bayesian Network.
- Parameter calibration: Applying PSO to optimize CPTs against expert-derived reference profiles to mitigate the parameterization gap.
- Multi-level analysis: Executing baseline risk quantification, path-level criticality analysis, and multi-faceted sensitivity testing.

This integrated approach ensures that the resulting systemic risk model is not only mathematically robust but also grounded in systems theory. The overall process is illustrated in Figure 1.

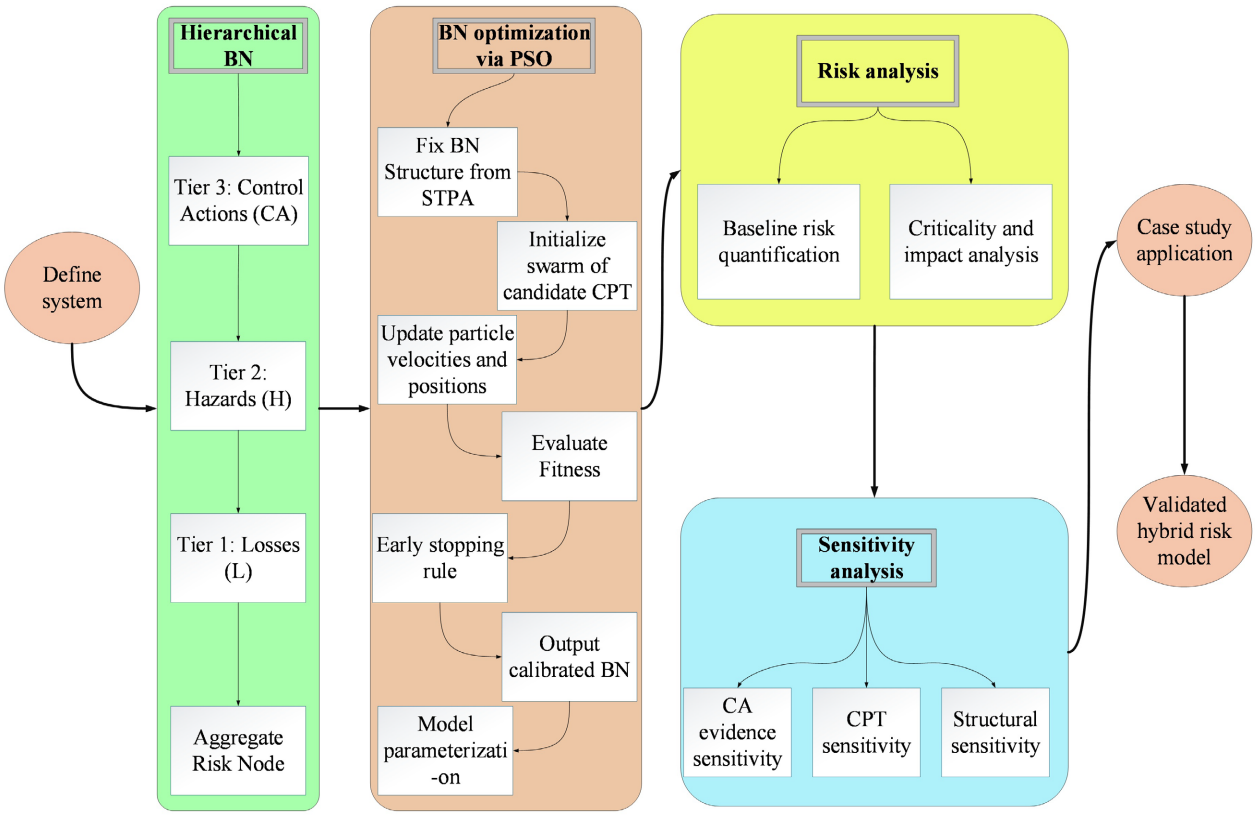


Figure 1. Methodology process.

3.1. Hierarchical BN Model Formulation

The foundation of the methodology is a three-tiered BN. To maintain logical consistency across the network, all variables follow a "failure-positive" polarity. In this convention, the "True" or "High" state of any node represents an unsafe condition or a failure. For example, Tier 3 Control Actions are modeled such that "True" indicates an Inadequate Control Action (e.g., CA6 "True" signifies insufficient worker training), and Tier 1 Losses (L) follow the same logic.

This structure is built directly from the validated outputs of prior work [14] to ensure that the model is grounded in a systemic understanding. STPA is a systemic safety analysis method introduced by Leveson (2004) that frames accidents not as single-point failures, but as inadequate control of complex socio-technical systems. Rather than focusing on component reliability, STPA identifies unsafe control actions, the hazards they may trigger, and the losses they can lead to [49] [50]. The tiers are constructed from the bottom up and the directed arcs follow the STPA adjacency CA → H → L → Risk. This architecture ensures that the BN captures the propagation pathways of risk, rather than just isolated failure probabilities. To maintain mathematical consistency, the network is enforced as a Directed Acyclic Graph (DAG). This hierarchical structure is designed to reflect the Industry 5.0 focus on sociotechnical resilience, specifically capturing how human-centric control actions (Tier 3) influence technical hazards (Tier 2) and subsequent system-level losses (Tier 1).

3.1.1. Tier 3—Control Actions (CA)

The root nodes of the model represent specific, observable control action scenarios through which control over the manufacturing system may be lost. These nodes serve as the initiating events in the risk pathways. Because they are root nodes, they are defined by prior probability distributions. In this framework, these priors are derived from expert elicitation and STPA-defined control flaws.

3.1.2. Tier 2—Hazards (H)

The intermediate nodes represent system-level hazards. Each hazard node is connected to its contributing CAs according to the STPA-defined control structure. These nodes represent states of the system that, under specific environmental conditions, will lead to a loss. The strength of the relationship between control failures and hazard activation is captured probabilistically in the node's CPT, which is optimized during the calibration phase.

3.1.3. Tier 1—Losses (L)

The top-level nodes represent system-level losses. As with the hazards, each loss node is connected to the specific hazards that may trigger it. These links are fixed by the STPA results to preserve the causal logic of the system. The corresponding CPTs quantify the likelihood that a hazard manifests as a tangible loss (e.g., worker injury, financial stoppage, or data breach).

3.1.4. Tier 0 – Risk (R)

The terminal node provides an aggregate measure of system risk. To ensure the model remains fully probabilistic (addressing limitations of deterministic counts), the Risk node utilizes a weighted CPT. This probabilistic approach allows the model to account for differential severity among loss types, ensuring that safety-critical outcomes (e.g., worker injury) have a higher mathematical influence on the "High" and "Very High" risk states than lower-priority technical or equipment losses.

3.2. Bayesian Network Optimization via PSO

After fixing the BN structure from STPA adjacency (CA → H → L → Risk), the unknown parameters Θ within the CPTs for all Hazard and Loss nodes are estimated using PSO. This framework utilizes a systematic simulation protocol designed for the design and early integration phases, where historical failure data is unavailable. The protocol initializes CA priors using a tiered mapping of control degradation and defines a synthetic target risk distribution $P(R)_{target}$ as the optimization objective.

The PSO algorithm maintains a swarm of 50 particles. The calibration is driven by a multi-objective fitness function $F(\Theta)$, which minimizes the weighted Mean Squared Error (MSE) between the model's predicted risk and expert-derived synthetic profiles. These profiles serve as high-level reference targets, established through a consensus-based elicitation process to define the expected risk distribution of the system.

While the targets are expert-informed, the use of PSO systematizes the calibration process. By automatically reconciling thousands of low-level CPT entries with high-level systemic goals, the algorithm reduces parameterization bias and ensures that the resulting probabilities are mathematically consistent with the STPA-derived causal structure. To satisfy the probability simplex constraint, every CPT column is renormalized after velocity updates such that $\sum pi = 1$.

$$\text{Loss} = \alpha * \text{MSE}_{\text{CA}} + (1-\alpha) * \text{MSE}_{\text{Risk}} \tag{2}$$

$$F(\Theta) = \frac{1}{\text{Loss} + \varepsilon} \tag{3}$$

where:

- MSE_{CA} measures the deviation of the model's sampled root nodes from the STPA-derived priors.
- MSE_{Risk} measures the L_2 norm between the model's 5-level risk distribution and the synthetic target profile.
- α is a weighting coefficient set to 0.6, prioritizing the causal anchoring of root control actions.
- ε is a small constant to prevent division by zero.

To ensure statistical significance and suppress noise in the fitness landscape, marginal probabilities are estimated via Monte Carlo sampling with 20,000 iterations per evaluation. The algorithm employs an early-stopping criterion, where

optimization terminates if the global best fitness fails to improve for a predefined threshold of 50 consecutive iterations. By iteratively calibrating the CPTs to reconcile local control failures with global outcomes, the model captures how risk propagation pathways reorganize across diverse manufacturing layouts. This structured approach provides a proactive, logic-based assessment tool that identifies emergent vulnerabilities before the system is operational, filling the critical gap left by purely data-driven models that rely on retrospective history.

3.3. Model Parameterization and Quantification

After the BN is constructed and calibrated, a single terminal "Risk" node provides an aggregate measure of system risk with five discrete states: Very Low, Low, Medium, High, and Very High [5]. To ensure theoretical consistency and account for differential loss severity, the CPT of the Risk node is modeled probabilistically rather than as a simple deterministic count.

This probabilistic parameterization allows for the weighting of losses; specifically, safety-critical outcomes are assigned a higher conditional influence on the "High" and "Very High" risk states than lower-priority technical losses. For decision-making, these five states are categorized into Acceptable Risk (Very Low, Low, Medium) and Unacceptable Risk (High, Very High). This threshold can be adjusted based on the specific risk tolerance of an industrial application.

3.4. Risk Analysis

Once the BN model is calibrated, a multi-faceted risk analysis is conducted to extract actionable insights. This framework moves from high-level systemic assessment to the identification of specific critical components and propagation pathways.

3.4.1. Baseline Risk Quantification

The baseline risk profile is established through Monte Carlo inference using 20,000 iterations, ensuring statistical significance and a stable probability distribution for the terminal "Risk" node. This initial assessment is conducted without external evidence to characterize the inherent systemic risk during the design phase. By establishing this baseline, the framework provides a benchmark to evaluate how risk propagation pathways reorganize when control actions are modified. Within this model, "Unacceptable Risk" is quantified as the cumulative probability of the "High" and "Very High" states, serving as the primary metric for identifying systemic vulnerabilities before the system is operational.

3.4.2. Criticality and Impact Analysis

To identify the most significant contributors to risk, two forms of criticality are assessed. First, the Node-Level Systemic Impact (ΔRisk) is calculated by forcing a node (CA, Hazard, or Loss) to its True state and measuring the absolute increase in baseline risk. This identifies "risk amplifiers" within the system. Second, a Path-Based CA Impact analysis quantifies the total risk propagated through all down-

stream pathways originating from each specific control failure, providing a metric for prioritizing managerial interventions.

3.5. Sensitivity Analysis

To test the model's robustness and simulate the impact of real-world operational changes, three distinct sensitivity analyses are performed:

- CA evidence sensitivity: This analysis simulates targeted management interventions. By perturbing CA priors by ±10%, we evaluate how a marginal improvement (or degradation) in a control action—such as worker training or device calibration—shifts the overall systemic risk.
- CPT sensitivity: This gauges the local brittleness of the model. By scaling the conditional probabilities of Hazard/Loss relationships by ±10%, we identify which causal links have the most profound influence on risk propagation.
- Structural sensitivity: This evaluates the importance of the system's logic itself. Each edge in the STPA-derived structure is removed in turn (while preserving acyclicity) to quantify the leverage of specific parent-child dependencies on the final risk outcome.

3.6. Framework Validation via Case Studies

To evaluate the diagnostic power and adaptability of the STPA-BN-PSO framework, a validation strategy is implemented using three distinct manufacturing contexts. These scenarios include: 1) sequential assembly, 2) flexible job-shop, and 3) disassembly for recycling, are specifically selected to represent the human-centric sociotechnical systems central to Industry 5.0. Unlike traditional models focused on machine failure, this validation demonstrates the framework's ability to model the complex interplay between human operators and smart wearables during the design and early integration phases.

By applying the same 4-stage methodology to these diverse layouts, the study identifies how risk propagation pathways reorganize when the role of the human worker shifts from a fixed sequence to a flexible, decentralized task. This comparative approach validates the framework's capability to prioritize human safety and operational resilience, directly reflecting the pillars of Industry 5.0. Detailed descriptions of the case parameters and structural interdependencies, building on the foundational qualitative analysis from prior work [14] are provided in Section 4 to maintain a clear distinction between the proposed methodology and its practical application.

4. Results

The results are reported across three case studies representing distinct operational contexts: sequential assembly (Case 1), job-shop assembly (Case 2), and disassembly for recycling (Case 3). A common, hierarchical network structure, derived from an STPA, provides the foundational model for all three analyses. **Table 1** provides an overview of these contexts.

Table 1. Overview of three wearables integrated manufacturing contexts used for STPA-BN-PSO evaluation.

Feature	Case study 1	Case study 2	Case study 3
Operational context	Assembly line	Job-shop assembly	Disassembly line
Primary task	Sequential assembly of components from bins	Multi-step assembly of a custom structure	Sequential disassembly and sorting of components for recycling
Smart glasses usage	Display step-by-step assembly/disassembly instructions, and provide visual guidance		
Smart glove usage	Enhance precision in handling parts, apply correct force, and detect components		
Supporting equipment	Conveyor line, component bins	Tool cabinet, component bins, dolly, computer	Tool cabinet, storage bins, conveyor line

To ensure the replicability of the calibration process and address the query regarding variable identification, the standardized lists of Control Actions (CA), Hazards (H), and Losses (L) derived from the foundational STPA phase are presented in Tables 2-4. These tables represent the qualitative input variables that define the structural interdependencies for all three models.

Table 2. List of Control Actions (CA).

Code	Description	Code	Description
CA1	Calibration regulations	CA8	Wearable's programming
CA2	Data of materials and positioning	CA9	Smart glasses provide assembly/ disassembly instructions
CA3	Haptic feedback/light feedback	CA10	Smart gloves guide pressure feedback
CA4	Moving products with conveyor/dolly	CA11	Place and sort parts in storage bins
CA5	Provide maps and instructions from the supervisor	CA12	Plan of product/sequence
CA6	Worker training	CA13	Highlight the hazardous parts
CA7	Wearable's connections		

Table 3. List of Hazards (H).

Code	Description	Code	Description
H1	Harmful activities that may lead to a worker's injury or death	H6	Communication problem between departments
H2	Insufficient training of workers to work with wearables	H7	Data security problem
H3	Not providing the required materials and structure on time	H8	Damage to the product during the process
H4	Not providing precise and real-time data	H9	Release of harmful refrigerants due to improper disassembly
H5	Connection problem between wearables	H10	Incorrect sorting of hazardous and non-hazardous components, leading to environmental or safety risks

Table 4. List of Losses (L).

Code	Description	Code	Description
L1	Loss or injury to the worker	L4	Financial losses due to the line stoppage
L2	Loss or unacceptable damage to the product	L5	Loss of sensitive information
L3	Loss or unacceptable damage to wearables	L6	Environmental loss

4.1. BN Model Calibration and Baseline Assessment

The first stage of the quantitative analysis involved calibrating the Bayesian Network for each case study. As defined in the methodology, the model's structure was fixed by the STPA results, while the unknown CPTs were estimated using the PSO algorithm. To ensure transparency and statistical stability, the PSO parameters used for the calibration are summarized in Table 5.

Table 5. PSO calibration parameters.

Parameter	Value	Description
Swarm size (N)	50	Number of particles
Max iterations	200	Maximum optimization steps
Inertia weight (w)	0.9	Controls the impact of previous velocity
Cognitive constants ($c1$)	0.9	Weight of particle's personal best
Social constants ($c2$)	1.5	Weight of swarm's global best
Early stopping	50	Iterations with no improvement before termination
MC samples	20,000	Samples per inference for baseline stability

4.1.1. PSO Convergence and Stability Analysis

The PSO was configured with a population of 50 particles and an early-stopping criterion applied whenever the global best fitness failed to improve for 50 consecutive iterations. To evaluate the stability of the heuristic optimization, the calibration was validated through multiple independent runs. Figure 2 illustrates the convergence of the optimization process across the three case studies. In practice, the algorithm successfully converged in all three operational contexts, but with notably different convergence dynamics that reveal the probabilistic character of each system.

In Case 1, the optimizer began from a modest initial fitness of 336.6, quickly climbed to 3406.4 by iteration 2, and then plateaued for more than 20 iterations before reaching 3946.9 at iteration 41. Several incremental improvements followed, but a decisive phase of rapid gains began at iteration 81, where the fitness jumped to 9267.2, then to 12,850.1 at iteration 83, and finally stabilized at 22,876.8 by iteration 103.

In Case 2, the optimization trajectory displayed a similar stair-step character but with even more pronounced plateaus. Starting from 313.0, the global best fitness leapt to 2304.2 by iteration 3, then it reached 21,841.3 at iteration 22, and finally stabilized at 28,130.0 by iteration 70. Case 3, however, revealed a more

complex fitness landscape. Beginning from 341.2, the fitness rose through stable intervals—15,713.6 at iteration 45 and 23,541.4 at iteration 85—before a surge at iteration 178 increased the fitness to 31,073.2. This unique trajectory reflects the high dimensionality and non-linear interdependencies inherent in disassembly for recycling.

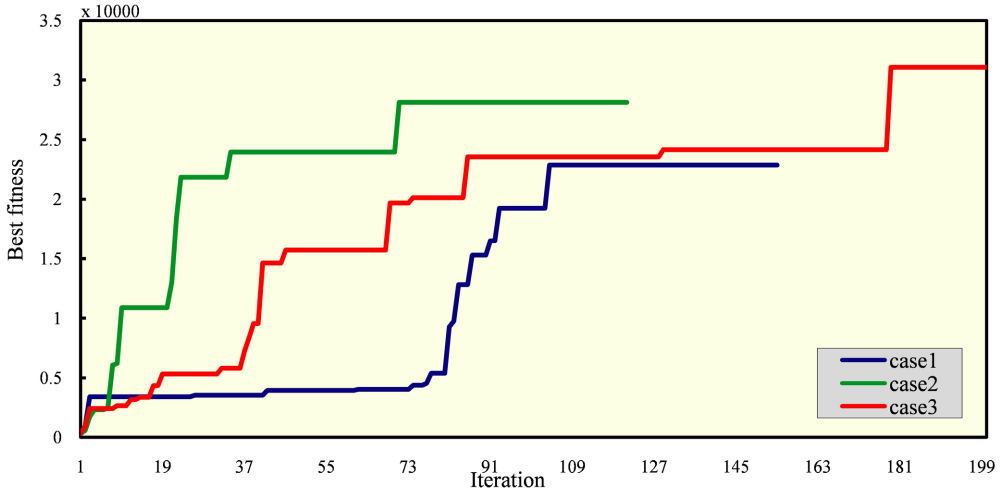


Figure 2. PSO convergence.

The observed stair-step character with pronounced plateaus and sudden surges in fitness across all cases can be attributed to the nature of the PSO algorithm interacting with a complex, multi-modal fitness landscape inherent in BN parameter learning. Specifically, particles may converge rapidly on local optima (explaining the plateaus) and only escape these through a global best update (explaining the sudden surges) that re-invigorates the swarm's exploration capabilities. The high consistency of these final fitness levels across multiple runs confirms the statistical stability of the framework.

The robustness of these convergence results is confirmed by the early-stopping criterion, where the optimization was only terminated after the global best fitness failed to improve for 50 consecutive iterations. This ensures that the final set of CPTs represents a state of mathematical equilibrium. Furthermore, the fact that the algorithm reached high fitness levels across three structurally different models demonstrates its reliability in reconciling the STPA control logic with the target systemic risk profiles. This internal consistency is vital during the design phase, as it confirms that the identified reorganization of risk pathways is not a mathematical artifact but a direct result of the framework successfully parameterizing the unique sociotechnical interdependencies of each operational layout.

4.1.2. Baseline Risk Quantification

Once calibrated, the CPTs were used to simulate baseline systemic risk distributions via Monte Carlo sampling (20,000 iterations). By utilizing a probabilistic terminal Risk node, the model reflects a safety-centric severity hierarchy where critical outcomes, such as worker injury (L1) and environmental loss (L6), are assigned higher

conditional weights than other technical losses. In a practical industrial application, these weights should be determined through a formal expert elicitation protocol or aligned with specific corporate risk-tolerance policies. However, for the purpose of this study, representative arbitrary weights were utilized to demonstrate the framework's robustness and its adaptive capability in prioritizing human-centric safety over purely technical or equipment-related failures.

Unacceptable risk is defined as the cumulative probability of "High" and "Very High" risk states. The baseline results, summarized in Table 6, show that the Job-Shop (Case 2) has the highest baseline level of unacceptable risk at 31.5%. This is followed closely by Disassembly Line (Case 3) at 30.7%, and the Assembly Line (Case 1) at 28.0%. A primary factor driving this increased risk is the significantly higher number of interconnections and dependencies within job-shop and disassembly processes; as these connections become more complex, the risk of systemic propagation grows substantially, which aligns with findings regarding the risk profiles of flexible manufacturing systems [51].

Table 6. Baseline risk profiles.

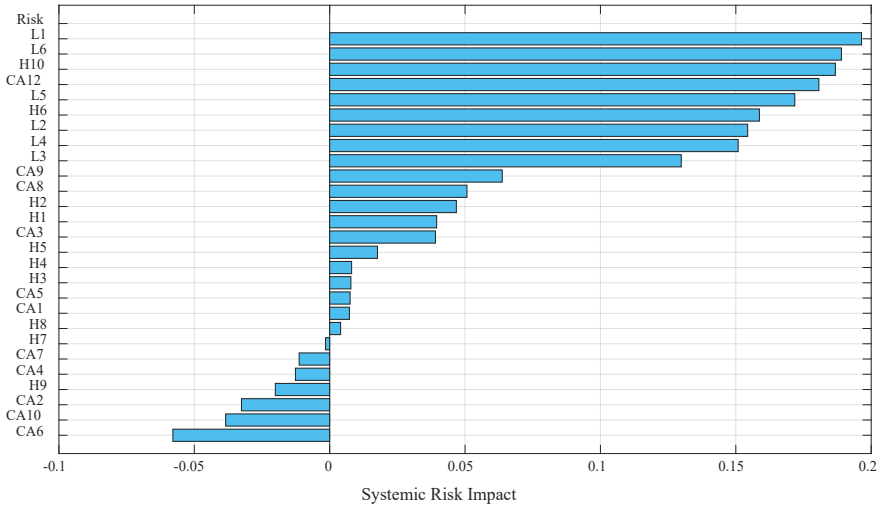
Case study	Very Low	Low	Medium	High	Very High	Unacceptable Risk: P(High + Very High)
Case 1	11.4%	20.1%	40.5%	19.3%	8.7%	28.0%
Case 2	10.4%	20.3%	37.8%	21%	10.5%	31.5%
Case 3	8.8%	19.9%	40.6%	20.0%	10.7%	30.7%

4.2. Risk Analysis

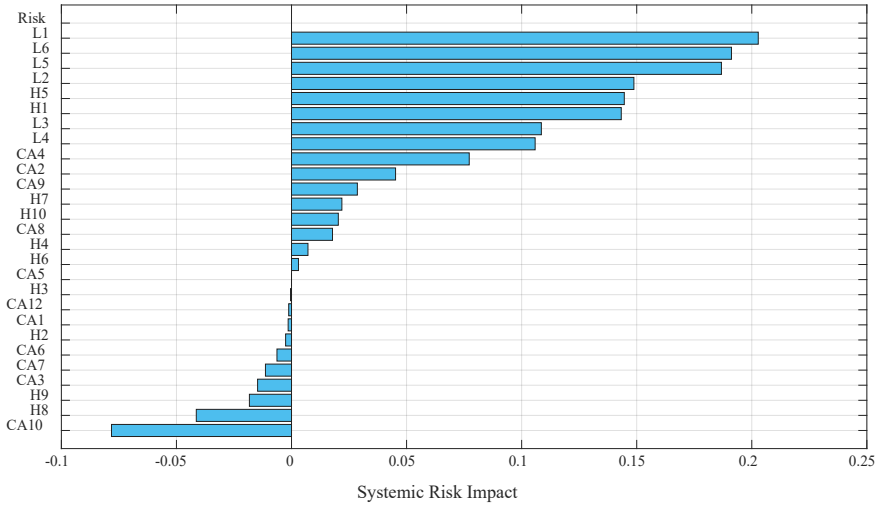
Following calibration, a multi-faceted risk analysis was performed on the three case study models to identify critical nodes and propagation pathways. Figure 3 illustrates the final criticality rankings (ΔRisk) of all nodes, showing how the marginal contribution of each control action (CA), hazard (H), and loss (L) changes the expected systemic risk when perturbed. The results reveal a strong context-dependence in risk drivers, reflecting the structural differences between sequential, flexible, and disassembly operations.

4.2.1. Node Criticality

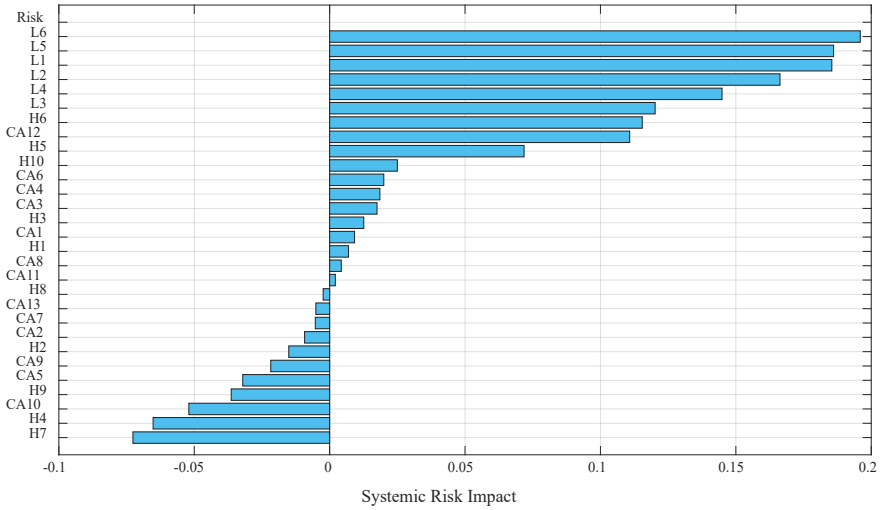
The implementation of the probabilistic weighted Risk node (as detailed in Section 3.3) allows the framework to prioritize safety-critical outcomes. In the sequential assembly case (Case 1), the most influential nodes are not limited to losses but include both control and hazard layers. Here, L1 (Worker injury, 0.196) and L6 (Environmental loss, 0.189) dominate the ranking. Their high scores are a direct result of the severity-weighting scheme, confirming that the model effectively prioritizes human safety. These are followed closely by H10 (Incorrect sorting, 0.187) and CA12 (Plan of product/sequence, 0.181). This indicates that risks in sequential operations are tightly coupled to planning quality, where even minor sequencing errors can cascade into immediate consequences for worker safety.



(a) Case 1



(b) Case 2



(c) Case 3

Figure 3. Final criticality ranking of all nodes.

Conversely, the job-shop case (Case 2) shifts the concentration of systemic risk toward the hazard layer, specifically those involving information flow and connectivity. The three most critical nodes are H4 (Lack of real-time data, 0.286), H5 (Wearable connection problems, 0.270), and H1 (Harmful activities, 0.269). This demonstrates that in flexible production contexts—central to Industry 5.0—unstable connectivity and poor data quality are the primary "risk amplifiers." In these decentralized layouts, the reliability of the Human-Machine Interface (HMI) is the most significant factor in maintaining system resilience.

The disassembly case (Case 3) reveals yet another shift: losses take precedence as the primary drivers of systemic vulnerability. L6 (Environmental loss, 0.196), L5 (Information loss, 0.186), and L1 (Worker injury, 0.186) top the ranking. The appearance of CA12 (Planning, 0.111) and H6 (Communication problems, 0.116) among the highest-ranked non-loss factors indicates that the inherent uncertainty of disassembly requires superior coordination to prevent the escalation of risk toward irreversible environmental or safety outcomes.

4.2.2. High-Risk Pathway Tracing

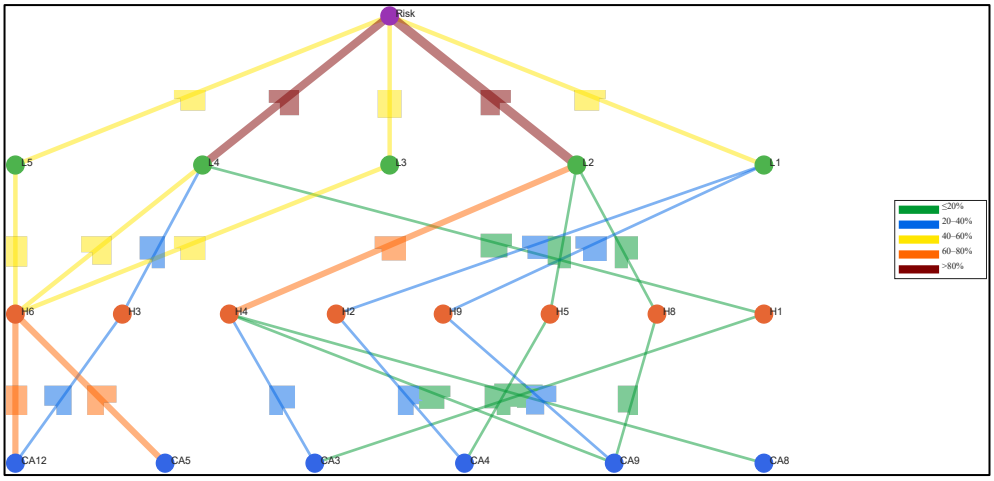
While **Figure 3** reports node-level systemic impact, **Figure 4** and **Figure 5** move to a path-level view. Specifically, **Figure 4** depicts the top control-to-loss routes (CA → H → L → Risk) as a risk-weighted network: edge thickness and color encode each route's contribution to expected severity. **Figure 5** lists the same top routes as a horizontal bar chart, giving their exact expected-severity values.

In sequential assembly, the dominant pathways originate from CA12 (Plan of product/sequence) and CA5 (Supervisor instructions), which channel risk through H6 (Communication problems) toward L5 (Information loss) and L4 (Financial losses). **Figure 5** confirms this pattern, with the highest bars corresponding to CA12 (Plan of product/sequence) and CA5 (Supervisor instructions)-driven routes, showing that even modest disruptions in planning and communication can cascade directly into significant financial and informational consequences.

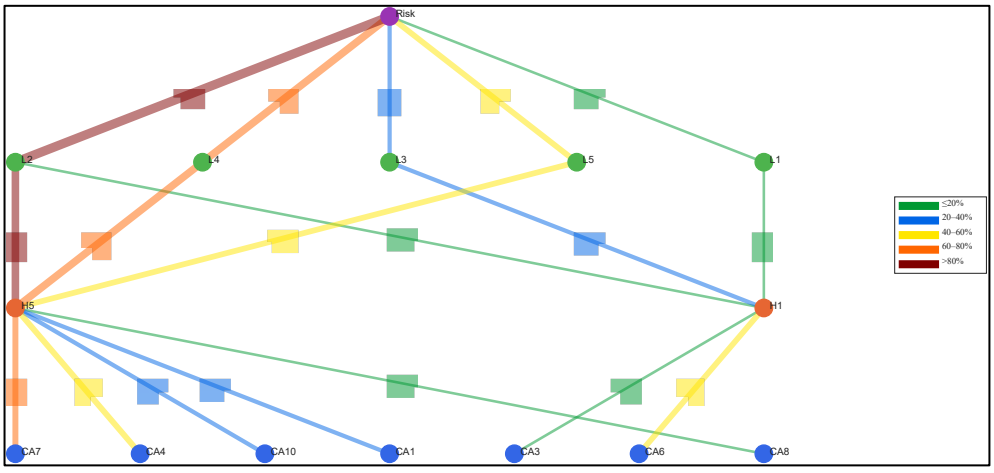
In the job-shop system, the dominant pathways originate from CA7 (Wearables' connections) and CA4 (Moving products with conveyor/dolly), which channel risk through H5 (Connection problem between wearables) toward L2 (Loss or unacceptable damage to the product) and L4 (Financial losses). This confirms that vulnerabilities in digital guidance and connection reliability create disproportionate impacts in flexible, decentralized production contexts.

In disassembly, the network maps and bar charts demonstrate that CA4 (Moving products with conveyor/dolly), CA7 (Wearable's connections), and CA3 (Haptic/light feedback) feed into H5 (Connection problem between wearables), H10 (Incorrect sorting of hazardous and non-hazardous components, leading to environmental or safety risks), and H1 (Harmful activities that may lead to a worker's injury or death), ultimately culminating in L2 (Loss or unacceptable damage to the product), L3 (Loss or unacceptable damage to wearables), L6 (Environmental loss), and L1 (Worker injury). Taken together, these figures highlight the context-sensitive nature of systemic risk and demonstrate the ability of the

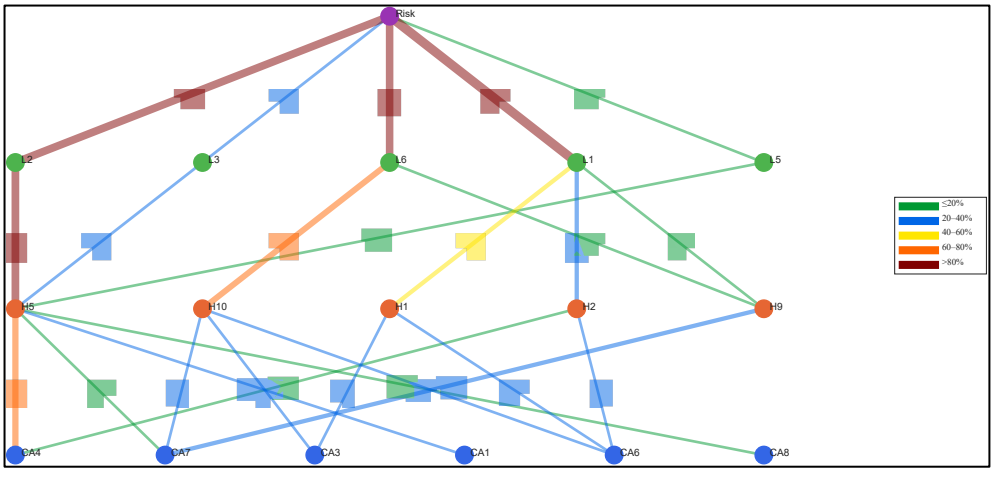
BN-PSO framework to uncover not only which nodes are critical but also how risks propagate through pathways to generate systemic vulnerabilities.



(a) Case 1

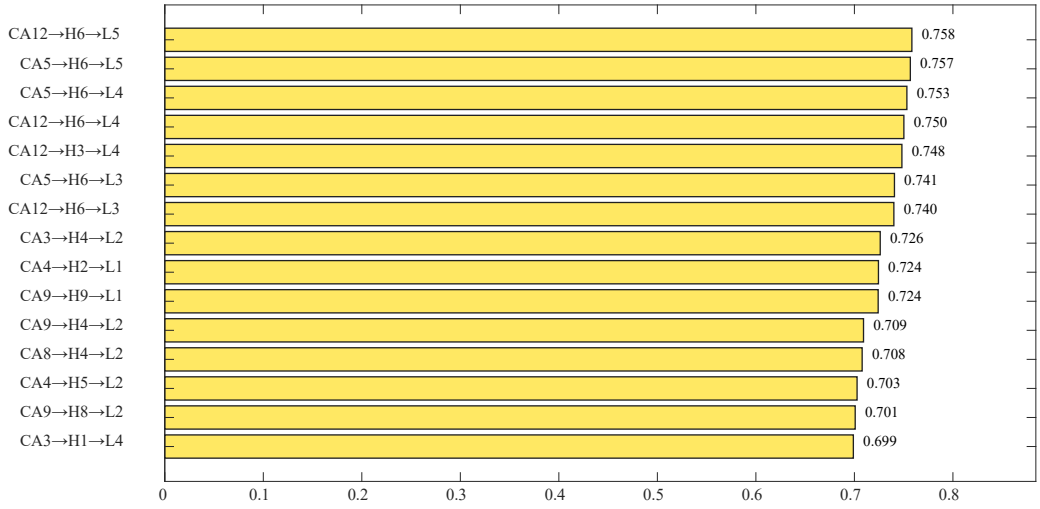


(b) Case 2

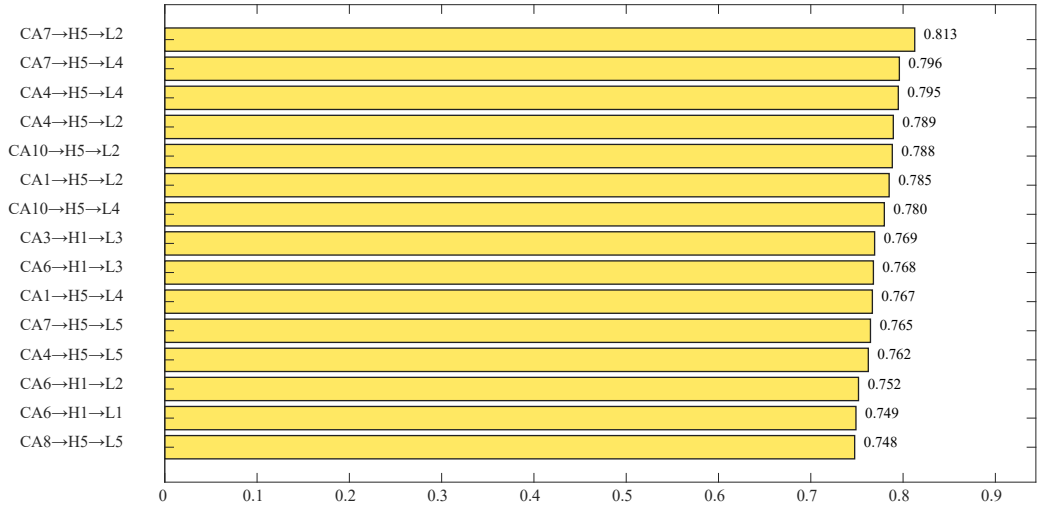


(c) Case 3

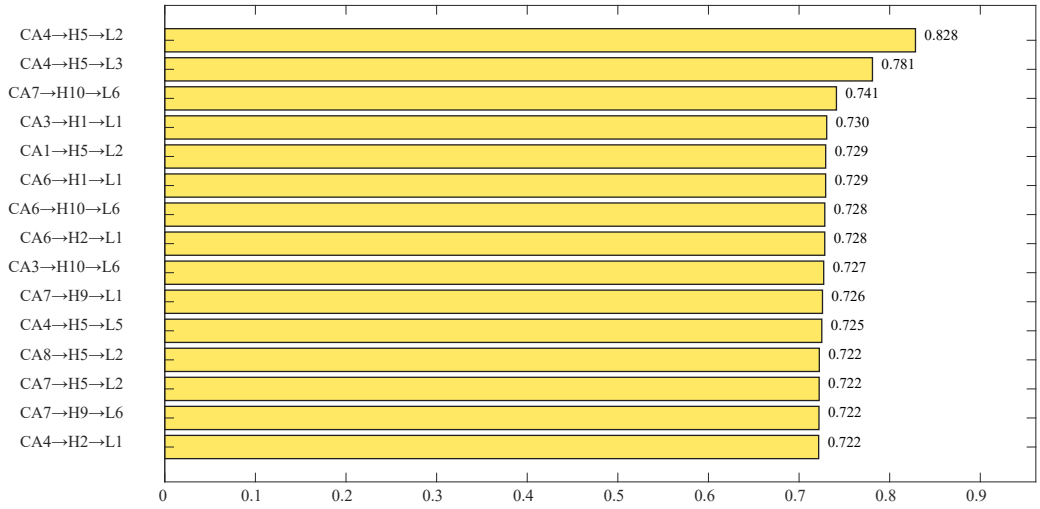
Figure 4. Risk-weighted paths network.



(a) Case 1



(b) Case 2



(c) Case 3

Figure 5. High-risk pathways sorted list.

4.3. Sensitivity Analysis

Building on the node and pathway-level findings, the final step examines how the network responds to perturbations in evidence, probability tables, and structural connections. This provides a comprehensive view of model robustness and systemic sensitivity, serving as a "what-if" simulation tool for managerial decision-support.

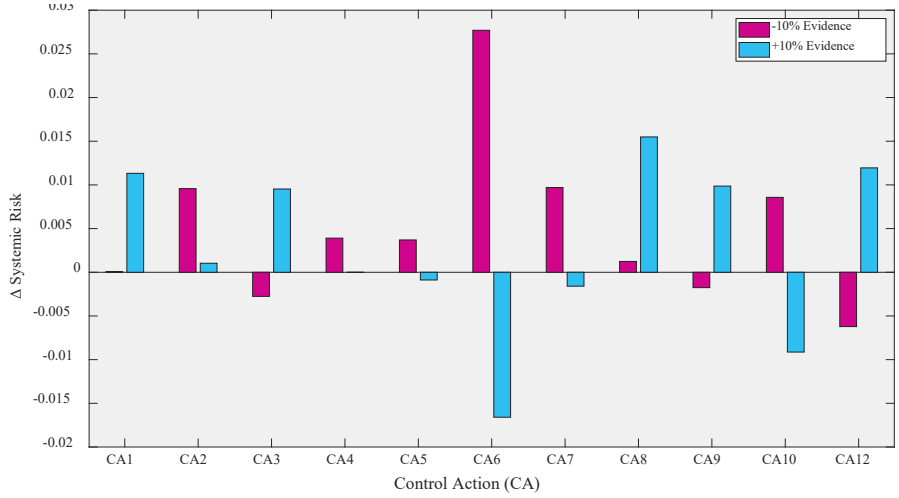
4.3.1. CA Evidence Sensitivity

The CA evidence sensitivity analysis is presented in Figure 6. These plots report how the expected severity of the Risk node changes when the marginal evidence for a given CA node is perturbed by +10% or –10%, holding the network structure and all CPTs fixed. In the panels, the blue bars correspond to a +10% increase in evidence for a given CA, and the pink bars represent a –10% decrease, with all other parts of the network held constant. Bars to the right indicate increases in expected severity (risk grows); bars to the left indicate decreases (risk falls).

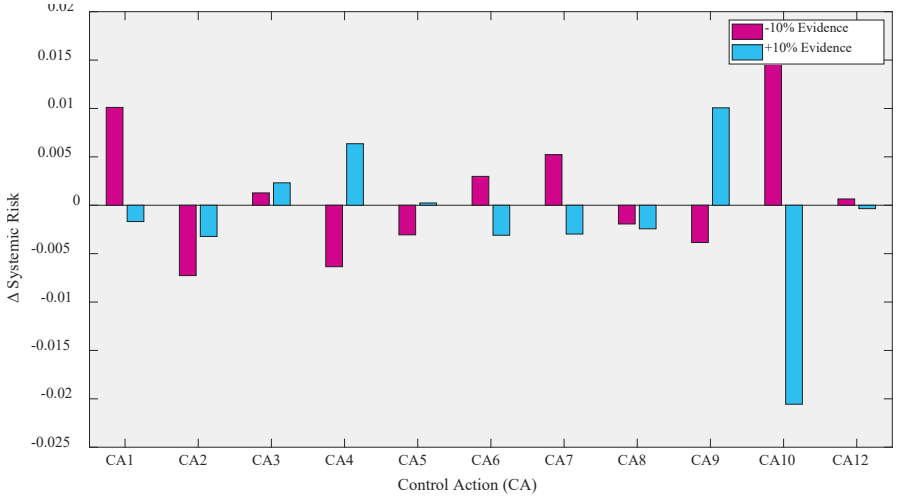
Whether the most influential bar sits on the +10% or –10% side depends on the role a CA plays at the operating point of the model. When a CA behaves like a driver of risk at baseline, adding evidence to it (blue) pushes the system toward more hazardous states and produces a larger positive shift. When a CA behaves like a barrier, removing evidence (pink) weakens protection and produces the larger increase in risk. In some cases, both bars point in the same direction; this occurs when small moves either way redistribute probability toward (or away from) the same high-impact routes because of interactions with competing paths.

In Case 1, the sensitivity analysis reveals that the system's overall risk is particularly influenced by a small subset of control actions, most notably CA6 (Worker training). This node demonstrates a pronounced asymmetry between positive and negative perturbations: when its probability is reduced by 10%, systemic risk rises sharply, whereas an equivalent increase leads to a notable risk reduction. This behavior suggests that CA6 (Worker training) serves a critical stabilizing function, absorbing uncertainty and maintaining system balance under normal operating conditions. Its sensitivity indicates that even minor degradation in its performance or reliability could propagate significant risk across the network. By contrast, control actions such as CA1 (Calibration regulations) and CA8 (Wearable's programming) also display noticeable sensitivities but in a direction that amplifies rather than mitigates systemic risk. Increasing their likelihood appears to exacerbate overall vulnerability, suggesting that their influence is more disruptive than protective.

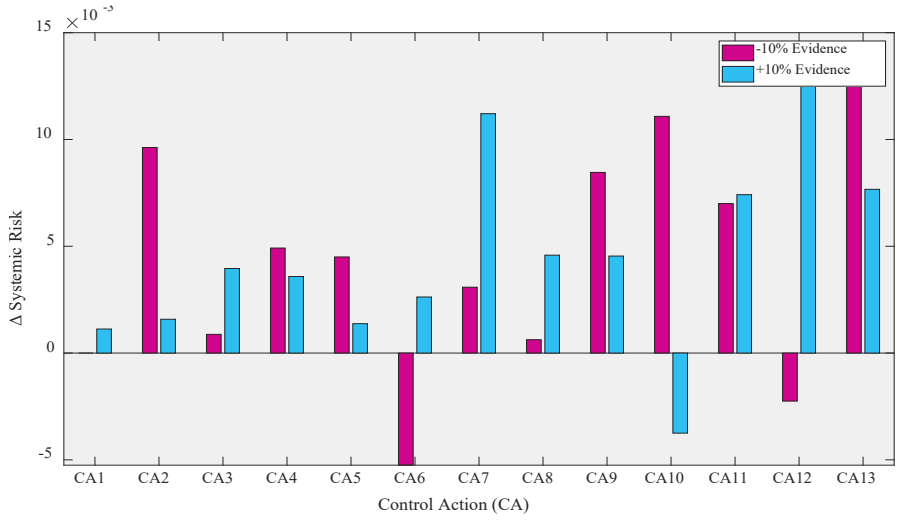
In Case 2, the sensitivity profile changes noticeably compared with the first scenario, showing that the propagation of risk depends strongly on the operational context. The most prominent variations appear around CA10 (Smart gloves guide pressure feedback), which produces the largest positive and negative deviations across all control actions. When the evidence supporting CA10 (Smart gloves guide pressure feedback) decreases by 10%, systemic risk increases sharply, while a 10% increase in its probability results in a marked reduction.



(a) Case 1



(b) Case 2



(c) Case 3

Figure 6. Sensitivity of systemic risk to CA evidence perturbation.

This clear asymmetry indicates that CA10 (Smart gloves guide pressure feedback) functions as a dominant protective mechanism in this configuration: its presence contributes to system stability, whereas its weakening immediately amplifies vulnerability. Moreover, CA1 (Calibration regulations), CA6 (Worker training), and CA7 (Wearable's connections) share a similar pattern: each shows a slight increase in systemic risk when their probabilities rise and a corresponding decrease when they are reduced, suggesting a moderate stabilizing effect whose influence is directionally consistent but less intense than that of CA10 (Smart gloves guide pressure feedback). In contrast, CA2 (Data of materials and positioning) and CA8 (Wearable's programming) display an opposite trend — both produce negative ΔScores under a −10% perturbation and minimal positive change under +10%, implying that these actions may exert a destabilizing or risk-amplifying influence when weakened.

In Case 3, CA13 (Highlight the hazardous parts) stands out as uniquely critical, exhibiting increased systemic risk under both positive and negative evidence perturbations, with the absence of evidence proving most detrimental. CA6 (Worker training) and CA12 (Plan of product/sequence) show a more complex behavior, where a reduction in evidence slightly decreases overall risk, suggesting that their activation may occasionally contribute to instability. By contrast, CA3 (Haptic feedback/light feedback), CA7 (Wearable's connections), CA8 (Wearable's programming), CA9 (Smart glasses provide assembly/disassembly instructions), and CA11 (Place and sort parts in storage bins) act as risk drivers, as greater evidence or confidence in their activation consistently corresponds to an escalation in systemic risk.

4.3.2. CPT Sensitivity

The CPT sensitivity analysis is presented in **Figure 7**. This analysis evaluates how variations in the CPTs of the Hazard and Loss nodes influence the expected severity of the Risk node. Each node's CPT was perturbed by ±10% while maintaining the original network structure and all other CPTs constant. In the panels, the light-blue bars represent a −10% scaling of the CPT values, and the black bars correspond to a +10% scaling. Bars extending to the right indicate an increase in expected severity (the system becomes more risk-prone), whereas bars to the left denote a reduction in systemic risk.

Because this procedure alters the underlying conditional dependencies rather than direct evidence, it highlights which Hazard and Loss relationships exert the greatest structural influence on the propagation of risk through the network. Nodes whose bars show large or asymmetric deviations reveal where small changes in local probability relationships can shift the global risk profile, identifying the most sensitive points in the model's internal logic.

For Case 1, H1(Harmful activities that may lead to a worker's injury or death) and H9 (Release of harmful refrigerants due to improper disassembly) exhibit the strongest positive deviations in Δ Systemic Risk, particularly under a +10% CPT scaling (black bars). This indicates that even small increases in the likelihood re-

lationships encoded in these nodes substantially raise the expected severity of the Risk node. Their sensitivity suggests that these hazards play a central role in transmitting or amplifying risk within the system structure. However, when their CPT values are reduced (–10%, light blue), H1 (Harmful activities that may lead to a worker's injury or death) shows a slight increase in risk, and H9 (Release of harmful refrigerants due to improper disassembly) demonstrates a modest increase. This observation reinforces their role as key contributors to upward risk propagation, suggesting that even a reduction in their internal probabilities does not mitigate risk, but rather maintains or slightly elevates it, confirming their critical nature as strong drivers. Among the Loss nodes, L4 (Financial losses due to the line stoppage) shows a similarly pronounced asymmetry: an increase in its CPT probabilities markedly elevates systemic risk, while a reduction produces only a minor mitigating effect. This asymmetric pattern implies that once a failure associated with L4 (Financial losses due to the line stoppage) becomes more likely, its downstream impact grows disproportionately—an indication of nonlinear risk amplification. Other nodes, such as H7 (Data security problem), H8 (Damage to the product during the process), L5 (Loss of sensitive information), and L3 (Loss or unacceptable damage to wearables), show moderate sensitivity, reflecting secondary effects on the overall risk balance.

In Case 2, the CPT sensitivity analysis reveals a more balanced yet directionally complex behavior across the Hazard and Loss nodes, suggesting that risk propagation in this scenario is shaped by intricate interdependencies rather than dominance by a few nodes, as observed in Case 1.

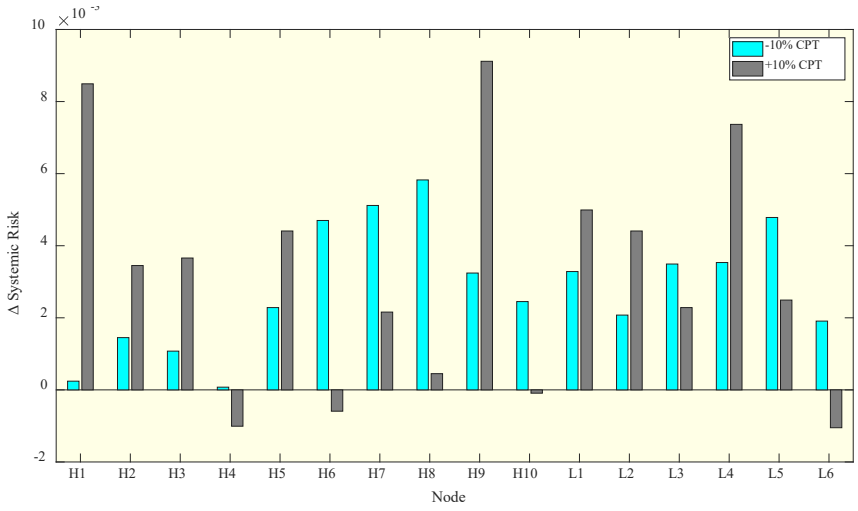
Among the Hazard nodes, H6 (Communication problem between departments), H7 (Data security problem), and H9 (Release of harmful refrigerants due to improper disassembly) stand out as the most influential. H7 (Data security problem) exhibits a substantial negative Δ Systemic Risk when its CPT values are increased, and a smaller positive effect when decreased. This asymmetry indicates that increasing the likelihood of H7's (Data security problem) causal relationships significantly reduces systemic risk, implying that H7 (Data security problem) functions as a critical mitigating mechanism—its integrity helps contain uncertainty in downstream pathways and actively reduces overall risk. Conversely, weakening its probabilities leads to a slight amplification of risk. H6 (Communication problems) shows a significant positive Δ Systemic Risk for both increased and decreased CPT values. This indicates that any perturbation to H6's (Communication problems) conditional probabilities, whether an increase or a decrease, leads to a substantial increase in systemic risk, making it a highly sensitive and volatile risk amplifier in this scenario. By contrast, H9 (Release of harmful refrigerants due to improper disassembly) demonstrates that a +10% increase in its CPTs elevates risk significantly, whereas a –10% decrease tends to reduce it. This analysis identifies its role as a risk-intensifying node, where stronger conditional links propagate instability through the network, but conversely, its mitigation can lead to a notable reduction in risk.

On the Loss side, L1 (Loss or injury to the worker) emerges as particularly sensitive. It exhibits the most extreme negative Δ Systemic Risk under –10% scaling, meaning that a small reduction in its conditional probabilities substantially lowers the expected severity. However, increasing its CPT reverses the effect, showing a significant increase in risk, confirming that L1 (Loss or injury to the worker) amplifies overall system vulnerability when its probabilities are strengthened.

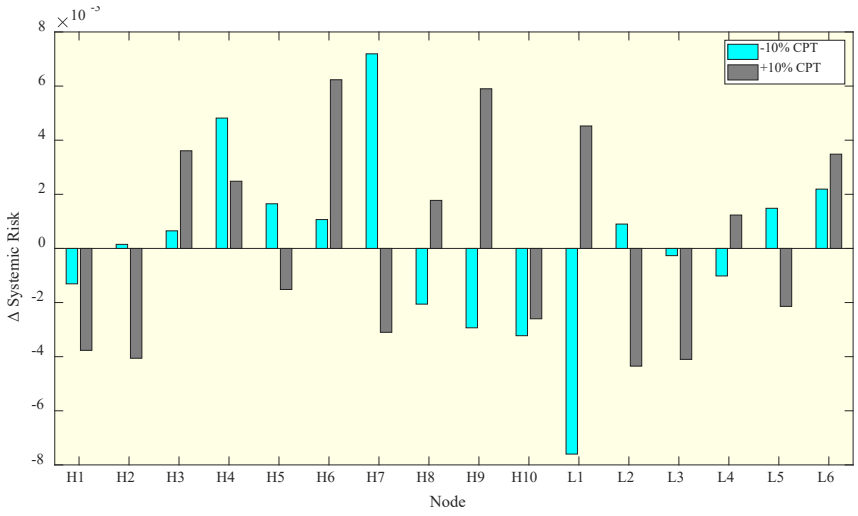
In Case 3, the CPT sensitivity analysis shows a broader and more amplified distribution of responses compared to previous cases, indicating that risk propagation is highly sensitive to changes in the conditional relationships among several Hazard and Loss nodes. Unlike the previous scenarios, where sensitivity was concentrated in a few elements, this case displays multiple high-impact nodes that collectively shape the systemic risk dynamics, often with asymmetric effects.

Among the Hazard nodes, H4 (Not providing precise and real-time data), H7 (Data security problem), H8 (Damage to the product during the process), and H9 (Release of harmful refrigerants due to improper disassembly) exhibit the most significant deviations. H8 (Damage to the product during the process) stands out as the most critical, demonstrating the highest positive Δ Systemic Risk under increased CPT scaling, implying that strengthening its conditional dependencies considerably increases systemic risk. Its sensitivity suggests that H8 (Damage to the product during the process) acts as a core amplifier—small probability increases in its hazard pathways have disproportionate effects on overall system severity. Similarly, H4 (Not providing precise and real-time data) and H7 (Data security problem) exhibit large positive shifts under decreased CPT scaling, indicating that reducing their CPT probabilities results in an escalation of risk. This pattern reflects their stabilizing function, as weakening these links reduces the model's ability to contain risk propagation toward severe loss states. H9 (Release of harmful refrigerants due to improper disassembly) demonstrates sensitivity in both directions, showing an increase in risk under both increased and decreased CPT scaling, implying a fragile equilibrium—any perturbation, whether amplification or reduction, destabilizes the system equilibrium.

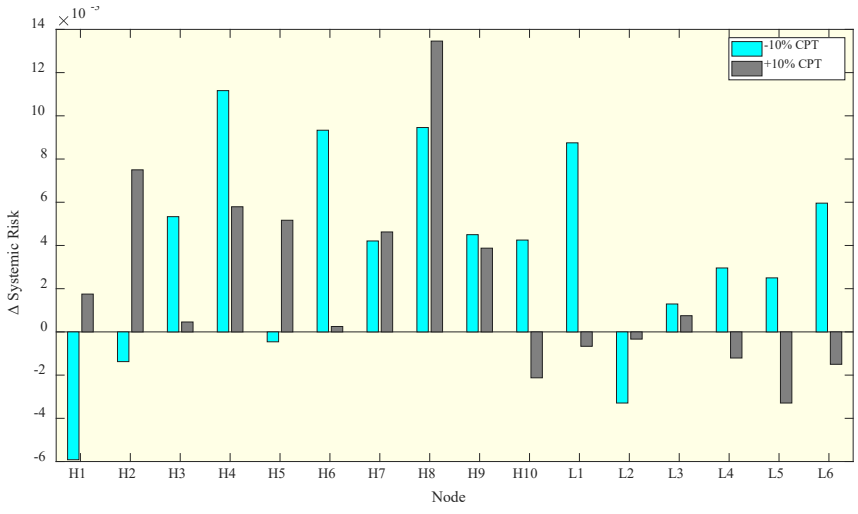
At the Loss level, L1 (Loss or injury to the worker), L5 (Loss of sensitive information), and L6 (Environmental loss) exhibit distinct but consistent patterns of asymmetry between the increased and decreased CPT perturbations. L1 (Loss or injury to the worker) shows a reduction in systemic risk when its CPT is decreased, with a negligible effect when increased. L5 (Loss of sensitive information), conversely, demonstrates an increase in systemic risk when its CPT is decreased, and a reduction when its CPT is increased. L6 (Environmental loss) similarly displays a pronounced increase in systemic risk under decreased CPT scaling, accompanied by a reduction under increased CPT scaling. These varied patterns indicate that changes in their CPTs induce specific directional shifts in systemic risk, though the overall magnitudes remain moderate compared to the primary Hazard nodes. This collective behavior suggests these nodes operate under related pathways or dependencies, contributing distinctively to the system's downstream response rather than acting as independent amplifiers.



(a) Case 1



(b) Case 2

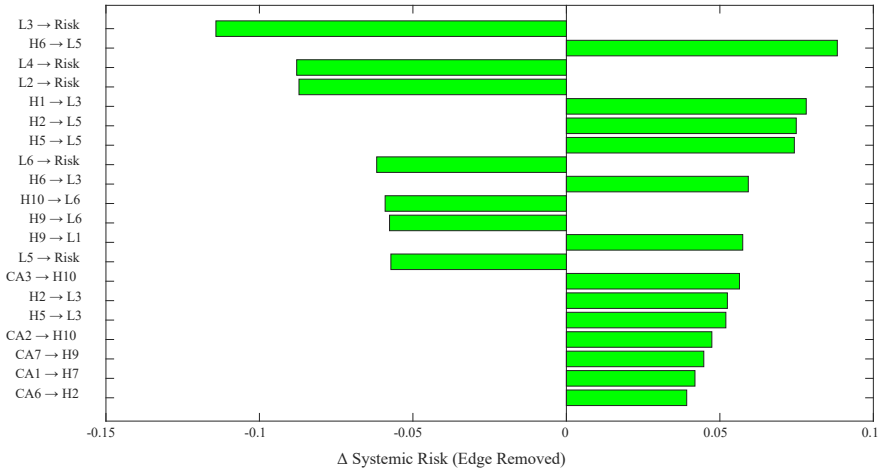


(c) Case 3

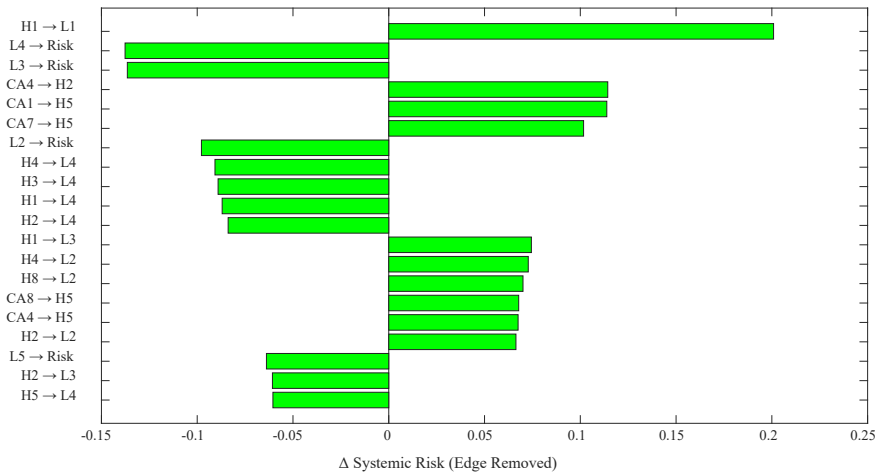
Figure 7. Sensitivity to CPT perturbation (hazards + losses).

4.3.3. Structural Sensitivity

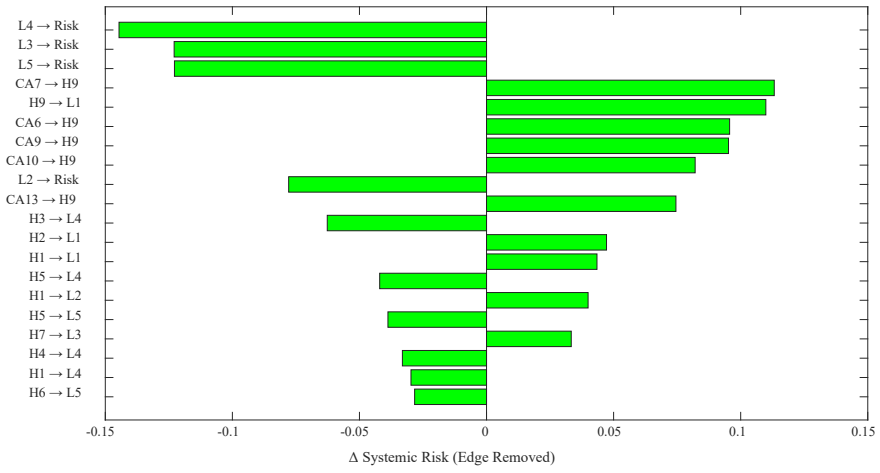
The structural sensitivity analysis evaluates how the network's topology—the



(a) Case 1



(b) Case 2



(c) Case 3

Figure 8. Top edges by structural impact.

presence of specific parent-child links—shapes overall risk. For each directed edge in the DAG, we evaluate its leverage by marginalizing the influence of the parent node on its child. This method allows the framework to quantify the impact of a specific causal dependency while preserving the mathematical integrity of the remaining CPT relationships. Positive values indicate that the link acts as a stabilizing coupling (protective), whereas negative values indicate the link functions as a risk-amplifying conduit.

Figure 8 reports the top 20 edges ranked by absolute impact (|ΔScore|) and visualized as green horizontal bars. This ranking surfaces the most consequential dependencies in the model—links whose presence or absence materially redistributes probability mass across high-severity routes. In practice, edges with large positive ΔScore are candidates for preservation or strengthening (they help contain escalation), while those with large negative ΔScore highlight amplifying pathways whose mitigation (through design changes, safeguards, or decoupling) can yield meaningful reductions in systemic risk.

In Case 1, the most influential structural dependencies appear among both Loss and Hazard pathways. A distinct pattern of significant risk amplification is observed for direct links from Loss nodes to the aggregate Risk node: L3 (Loss or unacceptable damage to wearables) → R, L4 (Financial losses due to the line stoppage) → R, and L2 (Loss or unacceptable damage to the product) → R all exhibit substantial negative Δ Systemic Risk upon removal. This indicates that these direct connections are strong amplifiers of systemic risk in the baseline configuration, and their removal substantially alleviates overall vulnerability. Other amplifying pathways include L6 (Environmental loss) → R, H10 (Incorrect sorting of hazardous and non-hazardous components, leading to environmental or safety risks) → L6 (Environmental loss), H9 (Release of harmful refrigerants due to improper disassembly) → L6 (Environmental loss), and L5 (Loss of sensitive information) → R, all showing notable reductions in systemic risk when removed.

On the other hand, a prominent group of edges, including H6 (Communication problem between departments) → L5 (Loss of sensitive information), H1 (Harmful) activities that may lead to a worker's injury or death → L3 (Loss or unacceptable damage to wearables), H2 (Insufficient training of workers to work with wearables) → L5 (Loss of sensitive information), and H5 (Connection problem between wearables) → L5 (Loss of sensitive information), yield substantial positive Δ Systemic Risk when removed. This indicates that these relationships serve as crucial protective couplings that help absorb uncertainty and limit escalation; eliminating them destabilizes the network and significantly increases overall risk. Other noteworthy protective links include H6 (Communication problem between departments) → L3 (Loss or unacceptable damage to wearables), H9 (Release of harmful refrigerants due to improper disassembly) → L1 (Loss or injury to the worker), CA3 (Haptic feedback/light feedback) → H10 (Incorrect sorting of hazardous and non-hazardous components, leading to environmental or safety risks), H2 (Insufficient training of workers to work with wearables) → L3 (Loss or unacceptable damage to wearables), H5 (Connection problem between wearables) → L3 (Loss

or unacceptable damage to wearables), CA2 (Data of materials and positioning) → H10 (Incorrect sorting of hazardous and non-hazardous components, leading to environmental or safety risks), CA7 (Wearable's connections) → H9 (Release of harmful refrigerants due to improper disassembly), CA1 (Calibration regulations) → H7 (Data security problem), and CA6 (Worker training) → H2 (Insufficient training of workers to work with wearables). These consistently positive values highlight the importance of these connections in maintaining safety boundaries and overall system resilience.

Case 2 exhibits several highly influential risk-amplifying pathways where edge removal leads to a substantial reduction in systemic risk. L4 (Financial losses due to the line stoppage) → R and L3 (Loss or unacceptable damage to wearables) → R stand out as the most critical amplifiers. These direct links from specific Loss nodes to the aggregate Risk node are identified as primary drivers of systemic vulnerability. Their removal demonstrates the greatest alleviation of overall risk, suggesting that these loss outcomes have a pronounced and direct impact on the system's severity assessment. Other significant amplifying connections include L2 (Loss or unacceptable damage to the product) → R, H4 (Not providing precise and real-time data) → L4 (Financial losses due to the line stoppage), H3 (Not providing the required materials and structure on time) → L4 (Financial losses due to the line stoppage), H1 (Harmful activities that may lead to a worker's injury or death) → L4 (Financial losses due to the line stoppage), H2 (Insufficient training of workers to work with wearables) → L4 (Financial losses due to the line stoppage), and L5 (Loss of sensitive information) → R.

In contrast, a set of edges acts as protective couplings, where their removal increases systemic risk, implying they help contain or channel risk in the baseline. The edge H1(Harmful activities that may lead to a worker's injury or death) → L1 (Loss or injury to the worker) shows the largest positive Δ Systemic Risk, indicating it is the most critical protective pathway in Case 2. Its presence is vital for managing H1's (Harmful activities that may lead to a worker's injury or death) influence, and its removal significantly destabilizes the network by allowing risk to propagate more freely or severely elsewhere. Edges linking Control Actions to Hazards are also prominent protective mechanisms: CA4 (Moving products with conveyor/dolly) → H2 (Insufficient training of workers to work with wearables), CA1 (Calibration regulations) → H5 (Connection problem between wearables), CA7 (Wearable's connections) → H5 (Connection problem between wearables), CA8 (Wearable's programming) → H5 (Connection problem between wearables), and CA4 (Moving products with conveyor/dolly) → H5 (Connection problem between wearables).

The consistent positive impact of removing these control action links underscores their fundamental role in restraining associated hazards (H2 (Insufficient training of workers to work with wearables), H5 (Connection problem between wearables)) and thereby mitigating systemic risk.

Case 3 demonstrates pronounced risk amplification through direct connections

from Loss nodes to the aggregate Risk node. L4 (Financial losses due to the line stoppage) → R, L3 (Loss or unacceptable damage to wearables) → R, and L5 (Loss of sensitive information) → R are identified as the most critical amplifiers. Their removal leads to the most significant reductions in systemic risk, indicating that these direct loss outcomes are primary drivers of overall system vulnerability. Another substantial amplifying pathway is L2 (Loss or unacceptable damage to the product) → R, reinforcing the pattern that direct propagation from various loss categories to the overall risk assessment significantly elevates systemic severity.

Conversely, a set of edges functions as crucial protective couplings, where their removal increases systemic risk, signifying their role in containing or channeling risk in the baseline. The most prominent protective links are those connecting Control Actions to Hazard nodes: CA7 (Wearable's connections) → H9 (Release of harmful refrigerants due to improper disassembly), H9 (Release of harmful refrigerants due to improper disassembly) → L1 (Loss or injury to the worker), CA6 (Worker training) → H9 (Release of harmful refrigerants due to improper disassembly), CA9 (Smart glasses provide assembly/disassembly instructions) → H9 (Release of harmful refrigerants due to improper disassembly), CA10 (Smart gloves guide pressure feedback) → H9 (Release of harmful refrigerants due to improper disassembly), and CA13 (Highlight the hazardous parts) → H9 (Release of harmful refrigerants due to improper disassembly).

The concentration of these control action links directed towards H9 (Release of harmful refrigerants due to improper disassembly) indicates that the system heavily relies on various control mechanisms to manage this specific hazard. Their consistent positive impact upon removal underscores their fundamental role in restraining H9 (Release of harmful refrigerants due to improper disassembly) and preventing broader risk escalation.

5. Discussion

A key contribution of BN lies in its ability to probabilistically capture how risks propagate across multiple system layers. Traditional risk analysis often stops at identifying unsafe control actions or hazards, but the hierarchical Bayesian Network allows dependencies to be represented explicitly and quantified through inference. The addition of PSO ensures that these probabilistic relationships are not arbitrarily assigned but are calibrated against both expert-driven priors (STPA-derived) and a plausible systemic risk profile. This dual mechanism strengthens the credibility of the resulting model and reduces reliance on subjective parameterization. One of the recurring challenges in systemic modeling is achieving a balance between transparency for decision-makers and quantitative robustness. STPA-BN-PSO addresses this tension by producing both numerical rankings and intuitive visualizations (e.g., path-weighted networks).

The results obtained across the three distinct case studies compellingly demonstrate the framework's adaptive diagnostic power. In the sequential assembly context (Case 1), systemic vulnerability was primarily centered around planning fail-

ures (CA12) and safety-critical losses. Conversely, in the job-shop environment (Case 2), communication and digital connectivity hazards (H6, H7) were identified as the primary drivers of risk. This reflects the increased complexity of the human-machine interface in decentralized layouts, where the reliability of information flow is the foundation of system resilience. Disassembly operations (Case 3), in contrast, revealed a convergence of multiple high-impact environmental (L6) and informational (L5) failures. These context-dependent shifts vividly illustrate the framework's ability to reveal how systemic risk reorganizes under varying operational conditions, providing a level of diagnostic detail that exceeds traditional linear methods.

From a managerial perspective, the STPA-BN-PSO framework offers several strategic advantages for proactive risk management. First, the baseline quantification revealed that nearly one-third of potential outcomes fall into unacceptable risk states, highlighting the urgency of mitigation during wearable deployment. Second, the criticality and path-based analyses provide a data-driven prioritization tool, allowing decision-makers to target the specific control actions that exert the most leverage on the final risk state. Third, the multi-layer sensitivity analyses serve as a "what-if" simulator. They empirically demonstrate that targeted interventions, such as improving worker training reliability (CA6), can yield disproportionate reductions in systemic risk. This alignment between model predictions and the structural logic of the manufacturing system enhances confidence in the framework's actionable recommendations.

Despite its strengths, the STPA-BN-PSO framework has several identifiable limitations. Its structural integrity is inherently tied to the initial STPA output; any omissions during the qualitative hazard identification phase will inevitably propagate into the quantitative BN model. Furthermore, while the PSO algorithm successfully systematizes the calibration process, it does not entirely eliminate subjectivity. The framework relies on expert-derived reference profiles to anchor the optimization, meaning that the resulting baseline risk estimates—such as the 31.5% unacceptable risk identified in the job-shop case—must be interpreted as scenario-conditioned benchmarks rather than absolute failure frequencies.

While this study utilized synthetic targets to demonstrate the stability and adaptive diagnostic power of the framework under data scarcity, future empirical validation using longitudinal industrial datasets is essential to confirm its external validity. The promising results point toward several high-impact directions for development. Integrating real-time sensor data from wearable devices directly into the BN priors could transform the framework from a design-phase assessment tool into a semi-autonomous monitoring system capable of adaptive, live risk assessment. Finally, coupling the STPA-BN-PSO methodology with multi-criteria decision-making (MCDM) would allow practitioners to balance safety-critical risk mitigation with broader organizational, economic, and sustainability priorities, fully realizing the pillars of Industry 5.0.

A direct quantitative comparison with conventional methods like Fault Tree

Analysis or manual Bayesian Networks was excluded due to their inability to model sociotechnical feedback or predict how risk pathways reorganize during the design phase. Conventional tools are fundamentally linear and reductionist, designed for mechanical systems that can be easily decomposed into independent, analyzable components. However, the wearable-enabled environments central to Industry 5.0 are not decomposable in this manner; systemic risks emerge from the complex interactions between humans, software, and physical devices rather than isolated component failures. Furthermore, these traditional tools require historical failure rates that are inherently unavailable in data-scarce early integration stages. In contrast, the STPA-BN-PSO framework uniquely bridges qualitative control logic and probabilistic quantification, capturing the non-linear interdependencies and emergent vulnerabilities that standard linear frameworks are less suited to represent in such highly coupled systems.

Table 7. Hybrid risk management framework comparison.

Feature/Criterion	STPA-PSO	FRAM-PSO	STPA-BN-PSO
Focus	Identification and prioritization of unsafe control actions	Variability propagation and sustainability-driven mitigation	Probabilistic risk and path reorganization across CA-H-L-Risk layers
Limitations	Not capture probabilistic dependencies; High reliance on expert input; Can be time-consuming	High dependence on expert input for variability parameters; Subjectivity in defining damping/amplifying factors	Dependent on foundational STPA quality; Requires reference targets for calibration; Subjectivity in severity weighting
Best application stage	Early system design and safety validation	Both design and improvement stages, especially when sustainability is central	Design and early integration phases (proactive assessment)
Unique contribution	Semi-automated feedback loop for risk prioritization and mitigation	Integration of sustainability criteria into systemic risk optimization	Provides systemic, path-based quantification of risk reorganization in data-scarce environments
Computational effort	Moderate	High	Very high
Data acquisition effort	Requires UCA lists, probabilities, and impact ratings	Requires detailed function mapping, SPCs, and variability distributions	Requires structured reference risk profiles (simulated or expert-derived)
Expert elicitation	High (hazard/UCAs identification, impact weighting)	Very high (function definitions, variability values, SPC impacts, sustainability scoring)	High (STPA priors + some CPT calibration)
Risk estimation bias	Possible bias in weighting and expert-driven ratings	Subjectivity in expert scoring of SPCs and sustainability pillars	Possible bias from assumed reference profiles and assigned severity weights
Best situations for use	When early design or integration stages require systematic hazard identification and prioritization; best for preliminary safety engineering	When sustainability trade-offs are central, or when decision-makers must balance environmental, economic, and social objectives in risk mitigation	When historical failure data is unavailable (early design stage); suitable for safety-guided design and predicting path reorganization
Industrial suitability	Complex socio-technical sectors (aviation, healthcare, rail, defense) where unsafe control actions must be identified early	Manufacturing, recycling, logistics, or energy sectors under strong sustainability mandates	High-reliability industries where proactive, path-level diagnostic power and probabilistic evidence are essential

When placed in the broader context of hybrid frameworks, STPA-BN-PSO complements alternatives such as STPA-PSO and FRAM-PSO. As summarized in Table 7, each method offers a unique contribution: STPA-BN-PSO provides path-based, probabilistic quantification with path-sensitivity; STPA-PSO delivers an early-stage qualitative feedback loop; and FRAM-PSO integrates sustainability criteria into risk optimization.

Taken together, these methods form a layered strategy for Industry 5.0: STPA-PSO for qualitative hazard structuring, STPA-BN-PSO for proactive probabilistic quantification during the design and early integration phases, and FRAM-PSO for managing variability during continuous improvement. This toolkit allows practitioners to select the most appropriate method based on computational effort and industrial suitability. Specifically, the STPA-BN-PSO framework is uniquely suited for data-scarce environments at the design stage, where it provides the path-level diagnostic power necessary to predict how risk propagation pathways will reorganize before the system becomes operational. This fills a critical gap by allowing for safety-guided design in high-reliability industries where probabilistic evidence and systemic foresight are essential.

6. Conclusions

This study introduced the STPA-BN-PSO framework as a probabilistic approach for assessing and managing systemic risks associated with the integration of smart wearables in complex Industry 5.0 manufacturing environments. By leveraging STPA-derived causal structures and calibrating probabilistic relationships through PSO, the methodology provides a robust and interpretable tool for proactive risk quantification during the design phase, where historical failure data is inherently scarce.

The application of the framework across three distinct manufacturing case studies yielded several key findings:

- **Quantitative risk profiling:** The results demonstrate that systemic risk is profoundly context-dependent. The Job-Shop environment (Case 2) exhibited the highest baseline unacceptable risk at 31.5%, while the sequential assembly line (Case 1) showed a lower baseline of 28.0%. This highlights the increased vulnerability created by the complex interdependencies and connectivity requirements of decentralized Industry 5.0 layouts.
- **Adaptive diagnostic power:** The framework successfully identified shifting risk drivers across operational contexts. In sequential operations, risk is primarily driven by planning quality (CA12), whereas in flexible job-shops, digital connectivity and information flow (H4, H5) are the primary amplifiers of systemic vulnerability.
- **Technical stability and rigor:** The PSO calibration process proved to be statistically stable across multiple independent runs. This confirms that the framework reliably identifies consistent model parameters despite the high-dimensional uncertainty inherent in sociotechnical systems.

- **Prioritization of human safety:** By utilizing a probabilistic weighted Risk node, the framework successfully prioritized safety-critical outcomes over technical losses. This ensures that the resulting risk assessments are aligned with the human-centric philosophy of Industry 5.0.

While STPA-BN-PSO advances systemic risk modeling, limitations include the current reliance on synthetic reference profiles for initial calibration and the structural dependence on the initial STPA output. Future research should prioritize extending the framework to integrate real-time sensor data from wearables into the BN priors, move toward semi-autonomous decision-support, and explore hybrid approaches that incorporate multi-criteria decision-making for broader organizational priorities.

In summary, this research establishes the STPA-BN-PSO approach as a powerful and interpretable tool that uniquely equips organizations to anticipate, prioritize, and mitigate the complex systemic vulnerabilities inherent in wearable-enabled manufacturing. Positioned strategically alongside design-oriented tools like STPA-PSO and sustainability-focused methods like FRAM-PSO, STPA-BN-PSO fills a critical operational gap in a comprehensive, layered risk-management stack tailored for the evolving landscape of Industry 5.0.

Acknowledgements

This work is supported by the Natural Sciences and Engineering Research Council of Canada and École de technologie supérieure.

Conflicts of Interest

The authors declare no conflicts of interest regarding the publication of this paper.

References

[1] Nishar, S. (2023) Enhancing Operational Efficiency: Exploring the Integration of SOPs Using Virtual Reality and Smart Glasses Technology in Food Manufacturing. *Intelligent Control and Automation*, **14**, 37-44. https://doi.org/10.4236/ica.2023.143003

[2] Sun, Q., Zhou, H., Fu, R., Wang, C., Guo, Y., Lang, Y., *et al.* (2026) Human-Centered Technology for Human-Machine Collaboration Driving System: Design and Experiments. *Computers & Industrial Engineering*, **212**, Article 111739. https://doi.org/10.1016/j.cie.2025.111739

[3] Arcidiacono, G., Antonacci, A. and Antony, J. (2025) The R-Evolution of Lean Six Sigma from Industry 4.0 to Society 5.0: Excellence 5.0. *International Journal of Quality & Reliability Management*, **42**, 2328-2349. https://doi.org/10.1108/ijqrm-11-2024-0415

[4] Eko'ola, R.V. and Nadeau, S. (2025) Systematic Selection of Visual and Cognitive Assistive Equipment: The Case of Gas Turbine Assembly in Narrow Spaces. *Intelligent Control and Automation*, **16**, 80-109. https://doi.org/10.4236/ica.2025.163005

[5] Karevan, A. and Nadeau, S. (2024) A Comprehensive STPA-PSO Framework for Quantifying Smart Glasses Risks in Manufacturing. *Heliyon*, **10**, e30162. https://doi.org/10.1016/j.heliyon.2024.e30162

[6] Karevan, A. and Nadeau, S. (2023) The Role of Industry 5.0 in Reducing the Risk of Human Error in Manufacturing: A Critical Literature Review. *CIGI-QUALITA-MOSIM*, Trois-Rivières. https://doi.org/10.60662/00a1-5g45

[7] Tenholt, J., Adam, S., Laun, M., Schiefer, C., Terschüren, C., Harth, V., *et al.* (2023) Influences of Smart Glasses on Postural Control under Single- and Dual-Task Conditions for Ergonomic Risk Assessment. *Biomedical Engineering/Biomedizinische Technik*, **68**, 545-552. https://doi.org/10.1515/bmt-2022-0404

[8] Zhang, X., Schall, M.C., Chen, H., Gallagher, S., Davis, G.A. and Sesek, R. (2022) Manufacturing Worker Perceptions of Using Wearable Inertial Sensors for Multiple Work Shifts. *Applied Ergonomics*, **98**, Article 103579. https://doi.org/10.1016/j.apergo.2021.103579

[9] AlKhader, W., Jayaraman, R., Salah, K., Antony, J. and Omar, M. (2025) Transformations in Manufacturing Quality in the Industry 4.0 Era: A Semi-Centennial Review Using Latent Dirichlet Allocation. *Computers & Industrial Engineering*, **208**, Article 111340. https://doi.org/10.1016/j.cie.2025.111340

[10] Karevan, A. and Nadeau, S. (2025) Fostering AI-Human Collaboration in Industry 5.0 Manufacturing. In: *Springer Series in Design and Innovation*, Springer Nature Singapore, 457-463. https://doi.org/10.1007/978-981-96-8908-8_69

[11] Lin, K., Chien, C. and Kerh, R. (2016) UNISON Framework of Data-Driven Innovation for Extracting User Experience of Product Design of Wearable Devices. *Computers & Industrial Engineering*, **99**, 487-502. https://doi.org/10.1016/j.cie.2016.05.023

[12] Hulme, A., McLean, S., Dallat, C., Walker, G.H., Waterson, P., Stanton, N.A., *et al.* (2021) Systems Thinking-Based Risk Assessment Methods Applied to Sports Performance: A Comparison of STPA, EAST-BL, and Net-HARMS in the Context of Elite Women's Road Cycling. *Applied Ergonomics*, **91**, Article 103297. https://doi.org/10.1016/j.apergo.2020.103297

[13] Chakhrit, A., Benharkat, N.E.H., Guetarni, I.H.M., Guedri, A. and Chennoufi, M. (2025) A Literature Review of Risk Assessment Approaches in Failure Mode and Effects Analysis. *International Journal of Quality & Reliability Management*, **42**, 2415-2454. https://doi.org/10.1108/ijqrm-01-2025-0042

[14] Karevan, A. and Nadeau, S. (2026) Integrating Smart Glasses and Smart Gloves in Hybrid Assembly/Disassembly Systems: An STPA-Driven Semi-Automated Risk Management Tool. *Robotics and Computer-Integrated Manufacturing*, **100**, Article 103253. https://doi.org/10.1016/j.rcim.2026.103253

[15] Sun, J., Fang, H., Wu, J., Sun, T. and Liu, X. (2020) Application of Bayesian Belief Networks for Smart City Fire Risk Assessment Using History Statistics and Sensor Data. In: *Communications in Computer and Information Science*, Springer Singapore, 3-11. https://doi.org/10.1007/978-981-15-2810-1_1

[16] Micu, E.A., *et al.* (2024) A Probabilistic Digital Twin Model for Inland Waterway Transportation Systems Using Bayesian Networks. *7th Conference on Sustainable Mobility* (*CSuM*), September 2024, Karditsa. https://hal.science/hal-04686200/

[17] Aghabegloo, M., Rezaie, K., Torabi, S.A. and Yazdani, M. (2023) A Metaheuristic-Driven Physical Asset Risk Management Framework for Manufacturing System Considering Continuity Measures. *Engineering Applications of Artificial Intelligence*, **126**, Article 106789. https://doi.org/10.1016/j.engappai.2023.106789

[18] Zhao, W. and Xu, M. (2026) A Passenger Flow Congestion Propagation Bayesian Network Model for Urban Rail Transit Hubs. *Reliability Engineering & System Safety*, **266**, Article 111655. https://doi.org/10.1016/j.ress.2025.111655

[19] Liu, Q., Hu, W., Yang, K. and Yang, J. (2025) Risk Assessment of Urban Underground Logistics System Operations in Built-Up Areas: A Hybrid Fuzzy Bayesian Network and Machine Learning Approach. *Computers & Industrial Engineering*, **207**, Article 111295. https://doi.org/10.1016/j.cie.2025.111295

[20] Baglietto, E., Consilvio, A., Febbraro, A.D., Papa, F. and Sacco, N. (2018) A Bayesian Network Approach for the Reliability Analysis of Complex Railway Systems. 2018 *International Conference on Intelligent Rail Transportation* (*ICIRT*), Singapore, 12-14 December 2018, 1-6. https://doi.org/10.1109/icirt.2018.8641655

[21] Mukherjee, P., Patra, S.S., Samantaray, S., Barik, L. and Barik, R.K. (2022) SCSF: Supply Chain Sustainability Framework by Bayesian Theory and Markov Model for Risk Analysis. In: Bhateja, V., *et al.*, Eds., *Evolution in Computational Intelligence. Smart Innovation, Systems and Technologies*, Vol. 267, Springer Nature Singapore, 301-308. https://doi.org/10.1007/978-981-16-6616-2_28

[22] Chien, C. and Peng, J. (2024) Bayesian Inference for Multi-Label Classification for Root Cause Analysis and Probe Card Maintenance Decision Support and an Empirical Study. *Journal of Intelligent Manufacturing*, **36**, 1943-1958. https://doi.org/10.1007/s10845-024-02336-z

[23] Rathnakumar, R., Lu, X., Huang, J., Yan, H. and Liu, Y. (2026) Bayesian Entropy Neural Networks for Physics-Aware Prediction. *Reliability Engineering & System Safety*, **266**, Article 111575. https://doi.org/10.1016/j.ress.2025.111575

[24] Cao, X., Ren, L., Wang, X. and Sun, C. (2025) Path Re-Planning Method of Unmanned Underwater Vehicles Based on Dynamic Bayesian Threat Assessment. *Ocean Engineering*, **315**, Article 119819. https://doi.org/10.1016/j.oceaneng.2024.119819

[25] Tian, R., Wang, C., Ma, Z., Liu, Y. and Gao, S. (2022) Research on Vehicle-Cargo Matching Algorithm Based on Improved Dynamic Bayesian Network. *Computers & Industrial Engineering*, **168**, Article 108039. https://doi.org/10.1016/j.cie.2022.108039

[26] Gu, W., Qiu, J., Hu, J. and Tang, X. (2024) A Bayesian Decision Network-Based Pre-Disaster Mitigation Model for Earthquake-Induced Cascading Events to Balance Costs and Benefits on a Limited Budget. *Computers & Industrial Engineering*, **191**, Article 110161. https://doi.org/10.1016/j.cie.2024.110161

[27] Li, Y., Li, Y., He, Z., Li, L. and Niu, Z. (2025) Multi-Task Bayesian Network Learning with Heterogeneous Data Mode for Root Cause Analysis in Multi-Variety Small-Batch Manufacturing. *International Journal of Quality & Reliability Management*, **43**, 904-929. https://doi.org/10.1108/ijqrm-07-2025-0231

[28] Cobb, B. and Li, L. (2019) Bayesian Networks for Statistical Process Control with Attribute Data. *International Journal of Quality & Reliability Management*, **36**, 232-256. https://doi.org/10.1108/ijqrm-10-2017-0227

[29] Chang, P. (2024) A Path-Based Simulation Approach for Multistate Flow Network Reliability Estimation without Using Boundary Points. *Reliability Engineering & System Safety*, **249**, Article 110237. https://doi.org/10.1016/j.ress.2024.110237

[30] Sui, Z., Yuan, X., Cai, B., Ye, F., Duan, Q., Zhao, Z., *et al.* (2025) Integrated Bayesian and Particle Swarm Approaches for Enhanced Gas Leak Detection in Complex Commercial Structures. *Sensors*, **25**, 1481. https://doi.org/10.3390/s25051481

[31] Engelbrecht, A.P. (2007) Computational Intelligence: An Introduction. John Wiley & Sons. https://doi.org/10.1002/9780470512517

[32] Karevan, A., Tee, K.F. and Vasili, M. (2020) A Reliability-Based and Sustainability-

Informed Maintenance Optimization Considering Risk Attitudes for Telecommunications Equipment. *International Journal of Quality & Reliability Management*, **38**, 873-891. https://doi.org/10.1108/ijqrm-04-2020-0114

[33] Du, G., Liang, X., Ouyang, X. and Wang, C. (2019) Risk Prediction of Hypertension Complications Based on the Intelligent Algorithm Optimized Bayesian Network. *Journal of Combinatorial Optimization*, **42**, 966-987. https://doi.org/10.1007/s10878-019-00485-z

[34] Wu, M. and Jiang, W. (2025) Multi-Objective Optimization in High-Dimensional Patent Layout Using Deep Bayesian Network and Hybrid Algorithm. *Discover Computing*, **28**, Article No. 34. https://doi.org/10.1007/s10791-025-09531-3

[35] Abdelhafidh, M., Fourati, M. and Chaari, L. (2023) Dynamic Bayesian Network-Based Operational Risk Assessment for Industrial Water Pipeline Leakage. *Computers & Industrial Engineering*, **183**, Article 109466. https://doi.org/10.1016/j.cie.2023.109466

[36] Karevan, A. and Nadeau, S. (2025) FRAM-PSO: A Semi-Quantitative Framework Integrating Multi-Dimensional Sustainability Criteria. *Computers & Industrial Engineering*, **210**, Article 111560. https://doi.org/10.1016/j.cie.2025.111560

[37] Afenyo, M., Khan, F., Veitch, B. and Yang, M. (2017) Arctic Shipping Accident Scenario Analysis Using Bayesian Network Approach. *Ocean Engineering*, **133**, 224-230. https://doi.org/10.1016/j.oceaneng.2017.02.002

[38] Zhang, G. and Thai, V.V. (2016) Expert Elicitation and Bayesian Network Modeling for Shipping Accidents: A Literature Review. *Safety Science*, **87**, 53-62. https://doi.org/10.1016/j.ssci.2016.03.019

[39] Guo, Y., Jin, Y., Hu, S., Yang, Z., Xi, Y. and Han, B. (2023) Risk Evolution Analysis of Ship Pilotage Operation by an Integrated Model of FRAM and DBN. *Reliability Engineering & System Safety*, **229**, Article 108850. https://doi.org/10.1016/j.ress.2022.108850

[40] Sun, X., Hu, Y., Qin, Y. and Zhang, Y. (2024) Risk Assessment of Unmanned Aerial Vehicle Accidents Based on Data-Driven Bayesian Networks. *Reliability Engineering & System Safety*, **248**, Article 110185. https://doi.org/10.1016/j.ress.2024.110185

[41] Li, H., Ren, X. and Yang, Z. (2023) Data-Driven Bayesian Network for Risk Analysis of Global Maritime Accidents. *Reliability Engineering & System Safety*, **230**, Article 108938. https://doi.org/10.1016/j.ress.2022.108938

[42] Castillo, E., Calviño, A., Grande, Z., Sánchez-Cambronero, S., Gallego, I., Rivas, A., *et al.* (2016) A Markovian-Bayesian Network for Risk Analysis of High Speed and Conventional Railway Lines Integrating Human Errors. *Computer-Aided Civil and Infrastructure Engineering*, **31**, 193-218. https://doi.org/10.1111/mice.12153

[43] Huang, T., Xiahou, T., Mi, J., Chen, H., Huang, H. and Liu, Y. (2024) Merging Multi-Level Evidential Observations for Dynamic Reliability Assessment of Hierarchical Multi-State Systems: A Dynamic Bayesian Network Approach. *Reliability Engineering & System Safety*, **249**, Article 110225. https://doi.org/10.1016/j.ress.2024.110225

[44] Song, C., Zhang, Y. and Xu, Z. (2019) An Improved Structure Learning Algorithm of Bayesian Network Based on the Hesitant Fuzzy Information Flow. *Applied Soft Computing*, **82**, Article 105549. https://doi.org/10.1016/j.asoc.2019.105549

[45] Sun, B., Zhou, Y., Wang, J. and Zhang, W. (2021) A New PC-PSO Algorithm for Bayesian Network Structure Learning with Structure Priors. *Expert Systems with Applications*, **184**, Article 115237. https://doi.org/10.1016/j.eswa.2021.115237

[46] MacAllister, A., Kohl, A. and Winer, E. (2020) Using High-Fidelity Meta-Models to

Improve Performance of Small Dataset Trained Bayesian Networks. *Expert Systems with Applications*, **139**, Article 112830. https://doi.org/10.1016/j.eswa.2019.112830

[47] Meng, H., Hu, M., Kong, Z., Niu, Y., Liang, J., Nie, Z., *et al.* (2024) Risk Analysis of Lithium-Ion Battery Accidents Based on Physics-Informed Data-Driven Bayesian Networks. *Reliability Engineering & System Safety*, **251**, Article 110294. https://doi.org/10.1016/j.ress.2024.110294

[48] Karevan, A. and Nadeau, S. (2024) FRAM Effectiveness in the Era of Industry 4.0: A Dual Perspective Review. *Proceedings of the IISE Annual Conference and Expo* 2024, Montreal, 18-21 May 2024.

[49] Lu, X., Zeng, S., Guo, J., Deng, W., He, M. and Che, H. (2025) An Integrated Method of Extended STPA and BN for Safety Assessment of Man-Machine Phased-Mission System. *Reliability Engineering & System Safety*, **253**, Article 110569. https://doi.org/10.1016/j.ress.2024.110569

[50] Riccardi, L., Compare, M., Mascherona, R. and Zio, E. (2025) Structural Causal Modeling and STPA for the Risk Analysis of a Rail System Powered by H2 Fuel. *Reliability Engineering & System Safety*, **256**, Article 110758. https://doi.org/10.1016/j.ress.2024.110758

[51] Vidal, G.H., Coronado-Hernández, J.R. and Minnaard, C. (2022) Measuring Manufacturing System Complexity: A Literature Review. *Journal of Intelligent Manufacturing*, **34**, 2865-2888. https://doi.org/10.1007/s10845-022-01974-5